Design, Synthesis, and Biological Evaluation of a Series of Lavendustin A Analogues That Inhibit EGFR and Syk Tyrosine Kinases, as Well as Tubulin Polymerization

Fanrong Mu,[†] Stephanie L. Coffing,[†] David J. Riese II,[†] Robert L. Geahlen,[†] Pascal Verdier-Pinard,[‡] Ernest Hamel,[‡] Jill Johnson,[§] and Mark Cushman*[,†]

Department of Medicinal Chemistry and Molecular Pharmacology, School of Pharmacy and Pharmacal Sciences, Purdue University, West Lafayette, Indiana 47907, Screening Technologies Branch, Developmental Therapeutics Program, Division of Cancer Treatment and Diagnosis, National Cancer Institute, Frederick Cancer Research and Development Center, Frederick, Maryland 21702, and Developmental Therapeutics Program, Division of Cancer Treatment and Diagnosis, National Cancer Institute, National Institutes of Health, Rockville, Maryland 20852

Received September 5, 2000

A series of *N*-alkylamide analogues of the lavendustin A pharmacophore were synthesized and tested for inhibition of the epidermal growth factor receptor (EGFR) protein tyrosine kinase and the nonreceptor protein tyrosine kinase Syk. Although several compounds in the series were effective inhibitors of both kinases, it seemed questionable whether their inhibitory effects on these kinases were responsible for the cytotoxic properties observed in a variety of human cancer cell cultures. Accordingly, a COMPARE analysis of the cytotoxicity profile of the most cytotoxic member of the series was performed, and the results indicated that its cytotoxicity profile was similar to that of antitubulin agents. This mechanism of action was supported by demonstrating that most compounds in the series were moderately effective as inhibitors of tubulin polymerization. This suggests that the lavendustin A analogues reported here, as well as some of the previously reported lavendustin A analogues, may be acting as cytotoxic agents by a mechanism involving the inhibition of tubulin polymerization.

Introduction

The protein tyrosine kinases (PTKs) play critical roles in many of the signal transduction processes that control cell growth, differentiation, mitosis, and death. They are therefore important targets for the development of therapeutic agents for the treatment of diseases that are characterized by uncontrolled cell proliferation, such as cancer and psoriasis.[1−3] Fractionation of a butyl acetate culture extract from *Streptomyces griseolavendus* led to the isolation of the novel PTK inhibitor lavendustin A.[4] Structure **1** was proposed for lavendustin A on the basis of ^{1}H and ^{13}C NMR data, and this tentative assignment was confirmed by total synthesis.[4] Lineweaver−Burke analysis carried out in the presence of varying concentrations of ATP and the substrate indicated that the inhibition was competitive with respect to ATP and noncompetitive with respect to the substrate when tested on the epidermal growth factor receptor (EGFR) tyrosine kinase,[4] although subsequent studies showed that lavendustin A can function as a hyperbolic mixed-type inhibitor with respect to both ATP and substrate.[5] It was also determined that the lavendustin A fragment **2** was as potent as the parent compound **1**, suggesting that **2** is the biologically active "pharmacophore" of lavendustin A.

These initial reports have stimulated work on the synthesis of lavendustin A itself and the synthesis and biological investigation of a variety of lavendustin analogues.[6−15] The ester derivative **3** and the amide **4** were both found to compare favorably with the lavendustin A pharmacophore **2**. In particular, the ester **3** was as potent as **2** versus the EGFR tyrosine kinase in a cell-free assay, but **3** was more potent than **2** as an inhibitor of EGF-stimulated DNA synthesis in ER 22 cells.[10] Furthermore, the amide **4** was reported to be more potent than **2** as an inhibitor of EGFR tyrosine kinase in a cell-free system.[13] In view of these results, and as an extension of our earlier work on the solid-phase synthesis of lavendustin A and derivatives,[15] we decided to synthesize and evaluate a series of amide derivatives of lavendustin A having the general structure **5**. These compounds have been tested versus both the receptor PTK EGFR in BaF3 mouse lymphoid cells as well as the nonreceptor PTK Syk in a cell-free system. In addition, the new compounds in this series were evaluated as cytotoxic agents using a variety of cultured human cancer cell lines, and the cytotoxicity profile of at least one agent, **13b**, was found to be similar to that of antitubulin drugs when analyzed using the COMPARE algorithm.[16−18] Since the COMPARE program was developed as a predictor of mechanism of action, these results led to the hypothesis that the lavendustin

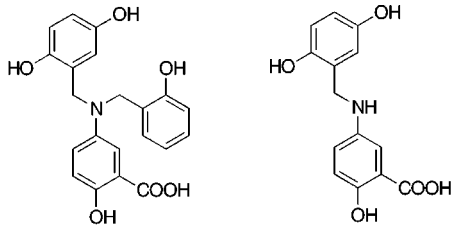

* To whom correspondence should be addressed. Tel: 765-494-1465. Fax: 765-494-1414. E-mail: cushman@pharmacy.purdue.edu.
[†] Purdue University.
[‡] Frederick Cancer Research and Development Center.
[§] National Institutes of Health.

10.1021/jm000387g CCC: $20.00
Published on Web 01/03/2001

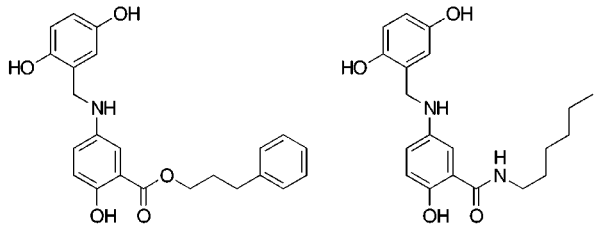

3

4

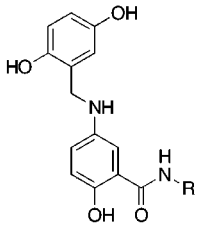

5

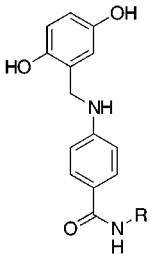

6

A analogues in our series were functioning as inhibitors of tubulin polymerization, and the appropriate assays were performed to test this hypothesis.

The COMPARE Algorithm

The COMPARE program was developed at the Developmental Therapeutics Program, National Cancer Institute (NCI), to interpret the emerging data from the 60-cell line in vitro human cancer cell cytotoxicity screen and display it in way that would facilitate comparison of the different patterns of dose−response curves produced by different cytotoxic agents. Paull and colleagues developed the "mean graph" representation of the screening data in which the mean concentration affecting all 60 cell lines at three levels of effect (GI_{50} = concentration causing 50% inhibition of growth; TGI = concentration causing total inhibition of growth; LC_{50} = concentration causing 50% cell kill) is plotted in the midline of the graph and the behavior of each individual cell line is represented as a deflection to the left for cells more resistant than the mean and to the right for cells more sensitive than the mean.[17] An important application of this manner of presentation is provided by the richly informative patterns of activity that emerge. Correlations of activity patterns can be quantified using a pattern recognition algorithm named COMPARE.[16] Use of the COMPARE program led to the realization that compounds with the same or similar mechanisms of action often result in cytotoxicity patterns that are similar.[16] This approach has resulted in identification of new tubulin polymerization inhibitors,[19] topoisomerase I and II inhibitors,[20,21] and dihydroorotate dehydrogenase inhibitors.[22] In another example, the use of COMPARE linked the effects of cucurbitacin[23] and jasplakinolide[24] to the actin cytoskeleton. Compounds with unique cytotoxicity profiles, suggesting modes of action not shared with the known clinically active classes of chemotherapeutic agents, have also been identified.[25]

A COMPARE analysis for a test agent can be run against the entire database of more than 77 000 compounds that have been tested in the NCI cell line cytotoxicity assay or against a database of standard agents whose mechanism of cytotoxicity is well-documented or against a single compound. The result of the analysis is a list of compounds in rank order and Pearson correlation coefficients, which provide an indication of the similarity of the patterns of cell line responses. Correlation coefficients of ≥ 0.60 are generally considered to be meaningful. For example, when a COMPARE is performed using paclitaxel as the seed, the correlation coefficient for vinblastine sulfate (another tubulin-interactive agent) is 0.88, whereas the correlation coefficient for phyllanthoside (a topoisomerase II inhibitor) is 0.422. The hypothetical mechanism of action suggested by COMPARE analysis can then be confirmed by laboratory testing. The reason that COMPARE analysis is a predictor of mechanism of action is that biological targets are expressed to a different extent in different cell lines, so that compounds which interact with a single biological target will have similar cytotoxicity patterns when tested in these cell lines.[26]

A COMPARE analysis was performed using **13b** as a seed. The top 20 compounds in the COMPARE analysis included 9 taxanes, 3 colchicine analogues, 2 combretastatins, and vinblastine, all of which interact with tubulin. Representative correlation coefficients between **13b** and various tubulin-interactive drugs were docetaxel, 0.790; vinblastine sulfate, 0.761; paclitaxel, 0.703; and maytansine, 0.701.

Synthesis

The synthesis of the series of lavendustin A analogues **13a**−**m** is a modification of a previously published route used to prepare a series of lavendustin A hydroxamic acid derivatives (Scheme 1).[10] Treatment of commercially available 5-aminosalicylic acid (**7**) with di-*tert*-butyl dicarbonate and triethylamine in aqueous dioxane afforded the Boc-protected intermediate **8**. Reaction of **8** with the appropriate primary amines **9a**−**m** in the presence of 1-(3-dimethylaminopropyl)-3-ethylcarbodiimide hydrochloride (EDCI), 1-hydroxybenzyltriazole hydrate (HOBt), and triethylamine in dry DMF yielded the series of amides **10a**−**m**. Deprotection of the intermediates **10a**−**m** with a mixture of dichloromethane and trifluoroacetic acid resulted in the formation of the primary amines **11a**−**m**. Reaction of **11a**−**m** with 2,5-dihydroxybenzaldehyde (**12**) afforded the corresponding Schiff bases, which were reduced with sodium cyanoborohydride to provide the desired lavendustin A analogues **13a**−**m**.

As outlined in Scheme 2, a variation of this route was executed in order to obtain the congeners **18a**−**c**, in which the aniline part of the molecule is substituted in the para position with various amides. Similarly, the lavendustin A analogue **23**, having a β-phenethylamide substituent in the meta position relative to the aniline nitrogen but lacking an adjacent phenolic hydroxyl group, was prepared as shown in Scheme 3.

Biological Results and Discussion

The lavendustin A analogues were examined for antiproliferative activity against the human cancer cell lines in the NCI cytotoxicity screen, in which the activity of each compound was evaluated using approximately 55 different cancer cell lines of diverse tumor origins. The mean-graph midpoint values (MGMs) listed in

Scheme 1

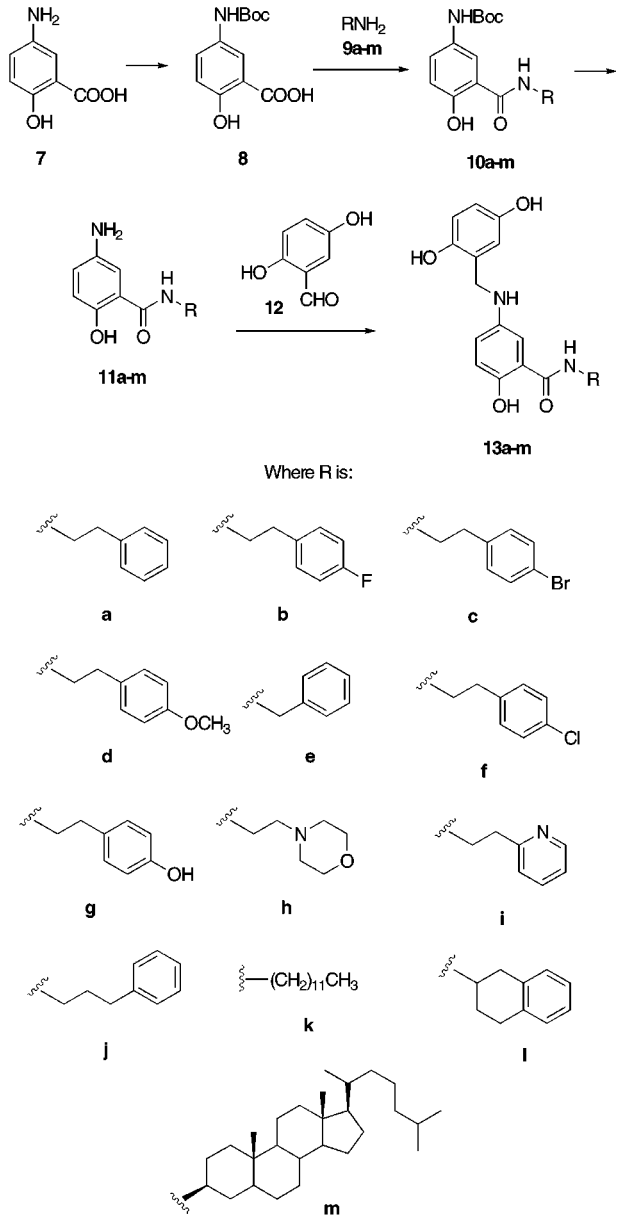

Scheme 2

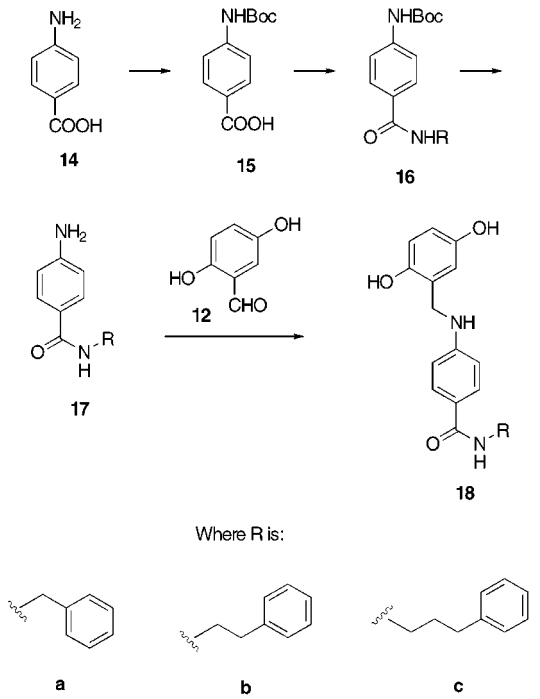

Scheme 3

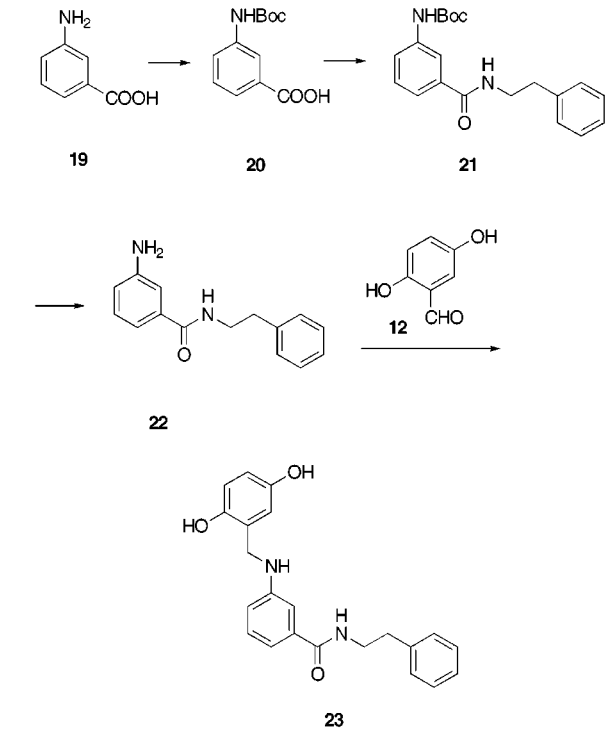

Table 1 are based on a calculation of the average GI_{50} values for all of the cancer cell lines tested (approximately 55) in which GI_{50} values below and above the test range (10^{-4}–10^{-8} M) are taken as the minimum (10^{-8} M) and maximum (10^{-4} M) drug concentrations used in the screening test.[18] A more detailed listing of the cytotoxicities of each compound in eight representative human cancer cell lines is presented in Table 2. With the exception of the cholestane derivative **13m**, all of the compounds in the series were found to be cytotoxic in human cancer cell cultures, with MGM values ranging from 0.35 to 20.4 μM. Starting with the basic β-phenylethylamine **13a**, which had an MGM of 14.8 μM, various substituents were introduced into the para position in order to determine how they affected cytotoxicity. The substituent that resulted in the greatest cytotoxicity was fluorine (**13b**, MGM 0.35 μM), followed by bromine (**13c**, MGM 7.6 μM), chlorine (**13f**, MGM 10.0 μM), methoxy (**13d**, MGM 15.4 μM), and hydroxy (**13g**, MGM 20.4 μM). Lengthening the chain of **13a** by one methylene unit had no appreciable effect on cytotoxicity (**13j**, MGM 13.2 μM), and shortening it by one methylene group also had little effect on cytotoxicity (**13e**, MGM 15.5 μM). The replacement of the benzene ring by a 2-pyridyl substituent (**13i**, MGM 16.0 μM) or a 2-tetralinyl substituent (**13l**, MGM 11.2 μM) did not result in any appreciable change in activity, while replacement of the benzene ring by a morpholine ring caused a slight decrease in cytotoxicity (**13h**, MGM 19.5 μM). The appendage of a long hydrocarbon chain to the amide in **13k** resulted in one of the more cytotoxic compounds (MGM 2.7 μM), but it was not an inhibitor of tubulin polymerization or Syk PTK (see below).

Table 1. Inhibitory Activities of Lavendustin A Analogues

	IC_{50} (μM)					
compd	MGM[a]	tubulin[b]	Syk[c]	EGFR[d]	MCF-7 DNA[e]	MCF-10A DNA[f]
4	8.7 ± 0.4	3.6 ± 0.7	NT[g]	14 ± 10	11 ± 4	14 ± 3
13a	14.8 ± 1.4	3.6 ± 1	5	10 ± 4	9 ± 3	11 ± 3
13b	0.35 ± 0.05	4.0 ± 0.4	5	4 ± 2	12 ± 4	10 ± 1
13c	7.6 ± 2.4	4.2 ± 0.5	45	35 ± 11	7 ± 0	6 ± 1
13d	15.4	4.2 ± 0.8	50	>100	14 ± 0	11 ± 2
13e	15.5	3.2 ± 0.6	25	8 ± 4	17 ± 4	17 ± 4
13f	10.0 ± 0.95	3.2 ± 0.7	25	46 ± 13	13 ± 2	9 ± 1
13g	20.4	4.5 ± 1	5	~300	16 ± 3	15 ± 2
13h	19.5	2.1 ± 0.4	1.5	>50	14 ± 3	16 ± 5
13i	16.0 ± 0.55	3.6 ± 0.3	NT[g]	15 ± 6	11 ± 5	7 ± 0.0
13j	13.2 ± 0.3	5.0 ± 1	28	1 ± 0.4	2 ± 0.2	2 ± 0.0
13k	2.7 ± 0.1	>40	50	35 ± 7	1 ± 0.3	3 ± 0.5
13l	11.2 ± 1.4	5.3 ± 0.9	8	4 ± 1	10 ± 3	6 ± 0.7
13m	>100	>40	NT[g]	*	>50	NT[g]
18a	8.8 ± 1.7	6.2 ± 1	18	>100	16 ± 3	34 ± 9
18b	6.4 ± 1.2	4.9 ± 0.9	5	>200	3 ± 1	7 ± 2
18c	5.3 ± 1.3	5.7 ± 1	35	33 ± 5	0.4 ± 0.1	3 ± 1
23	12.1 ± 0.8	6.9 ± 1	>100	~500	5 ± 1	6 ± 1

[a] Mean graph midpoint for growth inhibition of all human cancer cell lines (approximately 55) successfully tested. [b] IC_{50} values for inhibition of tubulin polymerization. [c] IC_{50} values for in vitro inhibition of Syk PTK. [d] IC_{50} values for inhibition of EGFR phosphorylation in BaF3 mouse lymphoid cells. [e] IC_{50} values for inhibition of DNA synthesis in MCF-7 cells. [f] IC_{50} values for inhibition of DNA synthesis in MCF-10A cells. [g] NT, not tested. [*] Stimulates EGFR tyrosine phosphorylation.

Table 2. Cytotoxicities of Lavendustin A Analogues in Human Cancer Cell Cultures

	GI_{50} (μM)[a]									
compd	leukemia CCRF-CEM	lung HOP-62	colon HCT-116	CNS SF-539	melanoma UACC-62	ovarian OVCAR-3	renal SN12C	prostate DU-145	breast MDA-MB-435	MGM[b]
4	0.56	19	17	2.3	12	4.0	6.1	15	15	8.7
13a	2.7	20	18	17	14	7.7	18	16	19	14.8
13b	0.29	12	9.2	9.2	7.8	11	7.7	18	13	0.35
13c	NT[c]	18	7.6	15.8	8.6	4.2	6.3	16	10	7.6
13d	3.2	12	23	16	14	5.5	72	21	16	15.4
13e	3.2	23	17	21	15	21	12	16	30	15.5
13f	1.6	17	15	8.4	13	5.9	9.8	16	20	10.0
13g	NT[c]	2.5	16	2.5	18	62	19	17	23	20.4
13h	1.8	NT[c]	20	19	17	87	22	17	13	19.5
13i	1.0	20	17	29	17	17	19	17	13	16.0
13j	2.4	22	24	16	14	6.5	15	8.4	18	13.2
13k	0.34	3.8	2.1	20	3.2	1.9	2.6	11	3.2	2.7
13l	1.4	17	16	2.7	14	7.9	18	17	9.2	11.2
18a	2.7	20	10	9.7	12	6.8	9.7	15	12	8.8
18b	0.59	13	7.4	8.5	9.4	2.7	7.4	14	5.1	6.4
18c	0.83	16	6.4	3.4	7.9	3.0	3.2	13	5.8	5.3
23	4.4	3.8	16	15	13	2.8	13	17	15	12.1

[a] The cytotoxicity GI_{50} values are the concentrations (μM) corresponding to 50% growth inhibition. [b] Mean graph midpoint for growth inhibition of all human cancer cell lines successfully tested. [c] NT, not tested.

Because the hydrocarbon chain in **13k** might be expected to be membrane-interactive, it was replaced by the cholestanyl moiety in **13m**, since that would be expected to bind strongly to biological membranes. However, the resulting compound **13m** proved to be inactive.

A series of analogues **18a**−**c** was designed by moving the amide to the para position and eliminating the phenolic hydroxyl group. The extension of the amide substituent by consecutive addition of methylene groups led to small increases in cytotoxicity (**18a**, MGM 8.8 μM; **18b**, MGM 6.4 μM; **18c**, MGM 5.3 μM). However, these small differences in cytotoxicity may not be significant based on the standard deviations reported. A final modification in this series involved the elimination of the phenolic hydroxyl group from **13a** (MGM 14.8 μM), resulting in **23** (MGM 12.1). Comparison of **13a** and **23** indicates that the phenolic hydroxyl group of **13a** is not a requirement for cytotoxicity.

Inhibition of EGF-stimulated EGFR phosphorylation by a number of the lavendustin A analogues was tested in BaF3 cells. After addition of inhibitor to the cells, they were stimulated by EGF under conditions which induce abundant receptor phosphorylation but not receptor downregulation or internalization.[27] Immunoprecipitates from the lysed cells were resolved by polyacrylamide gel electrophoresis and electrotransferred onto nitrocellulose. The resulting Western blots were probed with a mouse monoclonal antiphosphotyrosine antibody, and the bound antibody was detected by probing the blot with a horseradish peroxidase-coupled goat anti-mouse antibody. The antibody complexes were visualized by enhanced chemiluminescence. The resulting IC_{50} values for inhibition of EGFR phosphorylation are listed in Table 1. A total of 18 compounds were tested, of which 5 showed appreciable activity (IC_{50} 10 μM or less). The three most potent compounds were **13j** (IC_{50} 1 μM), having a γ-phenyl-

propyl substituent on the amide nitrogen, **13b** (IC_{50} 4 μM), having a *p*-fluoro-β-phenylethyl substituent, and **13l** (IC_{50} 4 μM), having a β-tetralinyl substituent. These three compounds were followed by the benzyl analogue **13e** (IC_{50} 8 μM) and the β-phenylethyl congener **13a** (IC_{50} 10 μM). Each of these values was relatively close to the IC_{50} values for inhibition of DNA synthesis in MCF-7 cells and MCF-10A cells (Table 1). Since MCF-10A cells are EGF-dependent, while MCF-7 cells are not, the fact that the two cell types exhibit similar responses to the lavendustin A analogues is evidence that inhibition of EGFR tyrosine kinase activity is not relevant to the cytotoxic activities of the lavendustin A analogues.[28−31] Compounds **13c**,**d**,**f**,**g**, **18c**, and **23** did not show appreciable activity versus EGFR tyrosine kinase at the concentrations tested.

To assay the new lavendustin A congeners versus a representative nonreceptor PTK, Syk was obtained from lysates of Sf9 cells infected with a baculovirus directing the expression of the full-length enzyme as a fusion protein with glutathione S-transferase. GST-Syk was isolated by affinity chromatography on glutathione-agarose. The activities of the inhibitors were assayed by monitoring the transfer of ^{32}P from [γ-^{32}P]ATP to tyrosyl residues on the immobilized kinase. Reactions were terminated by the addition of EDTA. The immobilized kinase was separated from unreacted [γ-^{32}P]-ATP by centrifugation. The extent of kinase autophosphorylation was determined by liquid scintillation spectrometry. The resulting IC_{50} values are listed in Table 1. In general, IC_{50} values for the inhibition of Syk were comparable to those obtained for the inhibition of EGFR. Four compounds (**13g**,**h** and **18a**,**b**), however, did display considerable selectivity for Syk as compared to the EGFR. These IC_{50} values are comparable to that of the Syk-selective inhibitor, piceatannol (**24**), which had an IC_{50} value of 5 μg/mL in this assay.

Whether or not the cytotoxicities of the lavendustin A analogues reported here are due to PTK inhibition is questionable. Since almost all of the EGFR tyrosine kinase activity must be inhibited before effects are seen on cell growth,[27] it is unlikely that the potencies of EGFR inhibitors seen here could possibly be responsible for the effects seen on inhibition of cancer cell growth, since the IC_{50} values for EGFR inhibition are close to the MGMs observed for growth inhibition. The fact that lavendustin A did not inhibit the PTK activity of the mutant protein pp60src^{F527}, but nevertheless did exhibit antiproliferative activity, previously led other investigators to the conclusion that the antiproliferative effects of lavendustin A could be due to actions on cellular targets downstream of pp60src^{F527} or receptors unrelated to the kinase.[11] We therefore also considered other possible targets for the new lavendustin analogues that might be responsible for their inhibitory effects on cancer cell growth.

As stated previously, the COMPARE analysis of **13b** suggested that the lavendustin A analogues in this series might be interacting with tubulin. As shown in Table 1, this turned out to be the case. All of the compounds except **13k**,**m** inhibited tubulin polymerization with IC_{50} values ranging from 2.1 to 6.9 μM. Under the reaction conditions used here, these values indicate the compounds are moderately active as inhibitors of the polymerization reaction. In previous studies under the same reaction conditions, known potent antimitotic agents such as combretastatin A-4 and dolastatin 10 reproducibly yield IC_{50} values in the 0.5−1.0 μM range. Compounds **4** and **13b**,**h** were also shown to be weak inhibitors of the binding of [^{3}H]colchicine to tubulin. In an assay with tubulin at 1 μM, [^{3}H]colchicine at 5 μM, and the three agents at 50 μM, the percent inhibitions for these compounds were **13b**, 38 ± 10%; **13h**, 34 ± 20%; and **4**, 45 ± 20%; as compared to 98 ± 2% with 5 μM combretastatin A-4 (**25**) (data not presented).

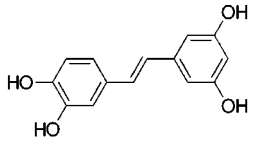

24

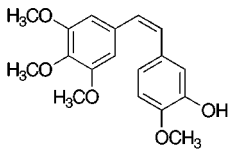

25

The activity of these compounds as inhibitors of tubulin polymerization was unexpected on the basis of prior literature reports, which have indicated that polyhydroxylated *trans*-stilbenes, benzylanilines, and related compounds are inhibitors of the PTKs, while their polymethoxylated *cis*-stilbene analogues and related compounds are inhibitors of tubulin polymerization. For example, in addition to lavendustin A and its analogues, other polyhydroxylated stilbene PTK inhibitors include piceatannol (**24**) and related polyhydroxylated *trans*-stilbenes,[7,32,33] while the polymethoxylated *cis*-stilbene inhibitors of tubulin polymerization include combretastatin A-4 (**25**) and its analogues.[34−37] Polymethoxylated *trans*-stilbenes are much less active as inhibitors of tubulin polymerization and as cytotoxic agents than their cis counterparts.[33] Neussbaumer et al. previously reported that the methylated lavendustin A analogues **26** and **27** have antiproliferative effects and that **27** acts "by blocking the cell cycle at mitosis by perturbing the microtubules of the mitotic spindle apparatus".[12,38] This would basically be in agreement with our prior study which had indicated that the benzylamine **28** and analogous compounds are antimitotic agents that act by inhibition of tubulin polymerization.[37] Furthermore, the methylated lavendustin A analogue **27** did not inhibit EGFR tyrosine kinase in a cell-free system.[38]

However, when we examined human Burkitt lymphoma cells treated with several members **(4**, **13b**,**c**,**e**,**f**,**k**, and **18a**−**c)** of this series of compounds for evidence of mitotic arrest (increase in G2/M cells), only **13b** caused such an effect. We thus have evidence for an antitubulin effect at the cellular level only with the most cytotoxic member of the series.

The abilities of the present polyhydroxylated benzylaniline derivatives of lavendustin A to inhibit both receptor and nonreceptor PTKs, as well as tubulin polymerization, is a novel observation which raises the possibility that the antiproliferative effects observed both in this series and in the other series of lavendustin A analogues reported in the literature may actually be due in part to inhibition of tubulin polymerization, rather than any effect on PTK inhibition. The lavendustin A derivatives reported are also unusual tubulin

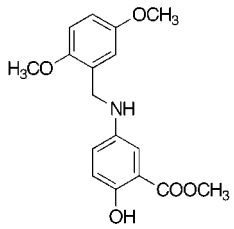

26

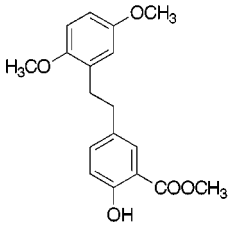

27

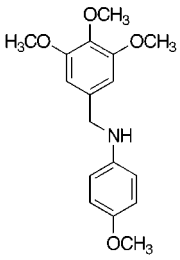

28

polymerization inhibitors, since they are not polymethoxylated *cis*-stilbene or benzylaniline analogues.

Experimental Section

General. Melting points are uncorrected. Nuclear magnetic resonance spectra for proton (^{1}H NMR) were recorded on a 300-MHz spectrometer. The chemical shift values are expressed in ppm (parts per million) relative to tetramethylsilane as internal standard; s = singlet, d = doublet, m = multiplet, bs = broad singlet. Microanalyses were performed at the Purdue Microanalysis Laboratory, and all values were within ±0.4% of the calculated compositions. Column chromatography was carried out using Merck silica gel (230−400 mesh). Analytical thin-layer chromatography (TLC) was performed on silica gel GF (Analtech) glass-coated plates (2.5 × 10 cm with 250 μm layer and prescored), and spots were visualized with UV light at 254 nm. Most chemicals and solvents were analytical grade and used without further purification. Commercial reagents were purchased from Aldrich Chemical Co. (Milwaukee, WI).

Tubulin Assays. Electrophoretically homogeneous tubulin was purified from bovine brain as described previously.[39] The tubulin polymerization and colchicine binding assays were performed as described previously,[40] except that Beckman DU7400/7500 spectrophotometers equipped with "high-performance" temperature controllers were used in the former assay. Unlike the manual control possible with the previously used Gilford spectrophotometers, the polymerization assays required use of programs provided by MDB Analytical Associates, South Plainfield, NJ, since the Beckman instruments are microprocessor-controlled. The Beckman instruments were unable to maintain 0 °C, and the lower temperature in the assays fluctuated between 2 and 4 °C. Temperature changes were, however, more rapid than in the Gilford instruments with the jump from the lower temperature to 30 °C taking about 20 s and the reverse jump about 100 s.

Syk Assays. Preparation of GST-Syk was as described previously.[41] Autophosphorylation reactions contained 50 mM Tris/HCl, pH 7.4, 5 mM $MnCl_2$, 5 μM ATP, 5 μCi [γ-^{32}P]ATP, 1 mM sodium orthovanadate, 5 mM *p*-nitrophenyl phosphate and 1.5% DMSO, which was used as a carrier for the inhibitors. Reactions were terminated by the addition of EDTA to a final concentration of 10 mM. Beads were washed 2 times in 50 mM Tris/HCl, pH 7.4, 1 mM sodium orthovanadate and 10 mM EDTA and counted by liquid scintillation spectrometry. IC_{50} values were determined graphically and represent the concentration of inhibitor that gives half-maximal inhibition as compared to control assays carried out in the absence of inhibitor but in the presence of DMSO carrier.

Cell Lines and Cell Culture. The CEM human T lymphocyte cell line engineered to express ErbB4 (CEM/4) and its culture conditions have been described previously.[42,43] Briefly, these cells were propagated in RPMI supplemented with 10% heat-inactivated fetal bovine serum and 300 μg/mL G418. The BaF3 mouse lymphoid cell lines engineered to express either EGFR (BaF3/EGFR) or ErbB2 and ErbB3 together (BaF3/2+3) and the culture conditions for these cell lines have been described earlier.[27] These cells were propagated in RPMI supplemented with 10% fetal bovine serum, 300 μg/mL G418, and 10% medium conditioned by WeHI cells. This conditioned medium serves as a source for interleukin 3.

MCF-10A human mammary epithelial cells and MCF-7, MDA-MB-231, and MDA-MB-453 human mammary tumor cell lines were obtained from the American Type Culture Collection (ATCC). These lines were propagated according to ATCC recommendations.

Inhibition of Receptor Tyrosine Phosphorylation Assay. The assay for inhibition of ErbB family receptor tyrosine phosphorylation was adapted from a previously described protocol.[27,43] Briefly, 200-mL cultures of CEM/4, BaF3/EGFR, or BaF3/2+3 cells were grown to saturation density (~10^6 cells/mL) and were incubated for 24 h at 37 °C in serum-free medium to reduce basal levels of receptor tyrosine phosphorylation. The cells were collected by centrifugation and resuspended in serum-free medium at a final concentration of ~10^7 cells/mL (~20 mL of cells). Cells were transferred to microcentrifuge tubes in 1-mL aliquots and putative kinase inhibitors were added to the cells. Each tyrosine kinase inhibitor was tested at 3−5 different concentrations. The inhibitors were dissolved in 5 μL of DMSO; hence, cells treated with 5 μL of DMSO were used as a solvent control. Cells were incubated in the presence of inhibitor for 2 h at 37 °C, then were incubated on ice for 20 min. Chilling the cells reduces the amount of ligand-induced receptor downregulation.[27]

Ligand was then added to the appropriate samples at a final concentration of 100 ng/mL and the samples were mixed and incubated on ice for 7 min. Recombinant human EGF (Sigma) was used as the ligand for EGFR, while neuregulin1β (NRG1β; R&D Systems) was used as the ligand for ErbB3 and ErbB4. Note that because ErbB3 lacks kinase activity, ligand-induced ErbB2 and ErbB3 phosphorylation in the BaF3/2+3 cells is the result of ErbB2 kinase activity.[27] Following incubation with ligand, the cells were collected by centrifugation, the supernatant was removed by aspiration, and the cells were resuspended in an isotonic lysis buffer containing 0.5% NP40/Igepal CA-630 (nonionic detergent; Sigma).

The cells were incubated for 20 min on ice to permit lysis. The samples were centrifuged for 10 min at 4 °C to collect the nuclei and cellular debris. The supernatants (cell lysates) were transferred to fresh tubes. Concanavalin A Sepharose (Amersham/Pharmacia) beads were added to each sample (35 μL of a 50% v/v slurry) and the samples were incubated at 4 °C for 30 min. Concanavalin A Sepharose precipitates the cellular glycoproteins, which include ErbB family receptors. The precipitated glycoproteins were washed 3 times with 500 μL of ice-cold lysis buffer, then were eluted by boiling the beads for 5 min in 80 μL of reducing SDS protein sample buffer. The beads were collected by centrifugation and one-half of the eluted glycoproteins (40 μL) were recovered and resolved by SDS/PAGE on a 7.5% acrylamide gel.

The resolved glycoproteins were electroblotted onto nitrocellulose (BiotraceNT; Gelman Sciences). The resulting blot was blocked by incubation for 45 min at room temperature in a solution consisting of 5% bovine serum albumin (Sigma) dissolved in Tris-buffered normal saline (TBS) supplemented with 0.05% Tween-20 (TBS-T). The blot was then probed with a mouse monoclonal antiphosphotyrosine antibody (4G10; Upstate Biotechnology). The blot was washed with TBS-T 5 times for 6 min each, and primary antibody binding was detected by probing the blot with a goat anti-mouse antibody conjugated to horseradish perioxidase (HRP; Pierce). The blot was washed with TBS-T 12 times for 10 min each, after which HRP activity was visualized by enhanced chemiluminescence (ECL; Amersham Pharmacia Biotech). The resulting chemilumigrams were digitized using a Linotype-Hell Jade flatbed

scanner and the amount of receptor tyrosine phosphorylation was quantified using NIH Image software. The amount of receptor tyrosine phosphorylation in samples from cells treated with a putative receptor tyrosine kinase inhibitor were compared to a standard curve generated using samples from cells treated with DMSO solvent control. This enabled us to determine the concentration of a given tyrosine kinase inhibitor that was necessary to cause a 50% reduction in receptor tyrosine phosphorylation. This value is reported as the receptor tyrosine phosphorylation IC_{50} value.

Inhibition of Cellular DNA Synthesis Assay. The assay for inhibition of cellular DNA synthesis was adapted from a previously described protocol.[44] Briefly, human mammary (tumor) cells were seeded in 1-mL aliquots into 24-well culture dishes at a density of 10^5 cells/well. Cells were incubated for 24 h at 37 °C, and a tyrosine kinase inhibitor dissolved in DMSO was added to each well in a volume of 10 μL. Each tyrosine kinase inhibitor was assayed at 3−5 different concentrations and each concentration was assayed using 3−4 wells of cells. Cells treated with 10 μL of DMSO served as the solvent control. Cells were then incubated for 48 h at 37 °C. [^{3}H]Thymidine (1.5 μCi; Amersham Pharmacia Biotech) dissolved in a 1.5 μL of an aqueous solution was added to each well and the cells were incubated for an additional 2 h at 37 °C. The culture medium was aspirated from the wells, and the cells were rinsed once with 1 mL of ice-cold phosphate-buffered saline (PBS) and once with 1 mL of ice-cold 10% trichloroacetic acid (TCA). Incorporated [^{3}H]thymidine was precipitated by incubating the cells for at least 30 min at 4 °C in 1 mL of 10% TCA. Following incubation, the TCA solution was aspirated from each well and the precipitated (incorporated) [^{3}H]thymidine was solubilized by incubating the cells for 30 min at 95 °C in 500 μL of 3% perchloric acid. The perchloric acid samples were transferred to scintillation vials containing 10 mL of Cytoscint scintillation cocktail (ICN). The incorporated [^{3}H]-thymidine was assayed by scintillation counting on a Packard Tricarb scintillation counter. The amount of [^{3}H]thymidine incorporation observed in the cells treated with the solvent control was divided by 2 (two) to determine the amount of half-maximal [^{3}H]thymidine incorporation. Dose−response curves for each combination of putative tyrosine kinase inhibitor and cell line were then constructed using the [^{3}H]thymidine incorporation data. The dose−response curves and the half-maximal [^{3}H]thymidine values were used to calculate the concentration of each inhibitor required to inhibit [^{3}H]thymidine incorporation by 50% in a given cell line. This value is reported as the DNA synthesis IC_{50} value.

5-[*N*-(*tert*-Butoxycarbonyl)amino]salicylic Acid (8). To a mixture of 5-aminosalicylic acid (**7**) (3.0 g, 19.6 mmol) in dioxane (50 mL) and water (25 mL) were added triethylamine (4.0 mL, 29.3 mmol) followed by di-*tert*-butyl dicarbonate (6.4 g, 29.3 mmol). The reaction mixture was stirred at room temperature for 24 h. Solvent was removed by rotary evaporation, and 3 N aqueous hydrochloric acid (30 mL) was added dropwise to the residue. A precipitate was obtained, collected, washed with water, and dried to provide **8** (4.76 g, 96%) as a solid: mp 279−280 °C; ^{1}H NMR (300 MHz, DMSO-d_6) δ 9.29 (s, 1 H), 7.96 (d, J = 1.81 Hz, 1 H), 7.47 (dd, J = 8.93, 2.69 Hz, 1 H), 6.85 (d, J = 8.88 Hz, 1 H), 1.44 (s, 9 H).

5-[*N*-(*tert*-Butoxycarbonyl)amino]-*N*-(β-phenethyl)salicylamide (10a). To a solution of **8** (1.5 g, 5.93 mmol) in dry DMF (15 mL) were added EDCI (1.71 g, 8.92 mmol), HOBt (1.2 g, 8.92 mmol) and triethylamine (1.65 mL, 11.86 mmol). After stirring at room temperature for 24 h, β-phenethylamine **(9a)** (3.7 mL, 29.5 mmol) was added dropwise and the reaction continued for 48 h at room temperature under argon. Water (300 mL) was then added and the mixture stirred for 5 min. The product was then extracted with ethyl acetate (5 × 50 mL). The combined organic extracts were washed with brine (1 × 40 mL), dried over sodium sulfate, filtered, and the solvent removed. Purification was achieved by flash chromatography (silica gel 75 g, ethyl acetate/hexane 1:4 by volume) to yield pure **10a** (1.09 g, 52%) as a white crystalline solid: ^{1}H NMR (300 MHz, $CDCl_3$) δ 12.13 (s, 1 H), 7.74 (s, 1 H), 7.36−7.24 (m, 6 H), 7.00 (dd, J = 8.82, 2.14 Hz, 1 H), 6.90 (d, J = 8.8 Hz, 1 H), 6.60 (bs, 1 H), 6.34 (s, 1 H), 3.68 (q, J = 6.859 Hz, 2 H), 2.93 (t, J = 7.1 Hz, 2 H), 1.51 (s, 9 H).

5-[*N*-(*tert*-Butoxycarbonyl)amino]-*N*-(4-fluoro-β-phenethyl)salicylamide (10b). From compound **8** (0.75 g, 2.9 mmol), EDCI (0.85 g, 4.5 mmol), HOBt (0.6 g, 4.5 mmol), triethylamine (1.65 mL, 11.8 mmol) and 4-fluorophenethylamine (**9b**) (1.2 g, 9.0 mmol), a similar procedure as that described for **10a** gave pure **10b** (0.58 g, 53%) as a white crystalline solid: mp 173−174 °C; ^{1}H NMR (300 MHz, DMSO-d_6) δ 11.68 (s, 1 H), 9.12 (bs, 1 H), 8.70 (t, J = 5.75 Hz, 1 H), 7.87 (s, 1 H), 7.28 (m, 3 H), 7.12 (t, J = 8.79 Hz, 2 H), 6.81 (d, J = 8.83 Hz, 1 H), 3.49 (q, J = 6.92 Hz, 2 H), 2.84 (t, J = 7.35 Hz, 2 H), 1.46 (s, 9 H).

5-[*N*-(*tert*-Butoxycarbonyl)amino]-*N*-(4-bromo-β-phenethyl)salicylamide (10c). From compound **8** (0.66 g, 2.6 mmol), EDCI (0.75 g, 3.9 mmol), HOBt (0.53 g, 3.9 mmol), triethylamine (1.45 mL, 10.4 mmol) and 4-bromophenethylamine (**9c**) (1.0 g, 5.0 mmol), a similar procedure as that described for **10a** gave pure **10c** (0.55 g, 49%) as a white crystalline solid: mp 196−197 °C; ^{1}H NMR (300 MHz, DMSO-d_6) δ 11.66 (s, 1 H), 9.13 (bs, 1 H), 8.71 (t, J = 4.99 Hz, 1 H), 7.81 (s, 1 H), 7.49 (dd, J = 8.20, 1.81 Hz, 1 H), 7.30 (d, J = 8.20 Hz, 2 H), 7.22 (d, J = 8.11 Hz, 2 H), 6.81 (d, J = 9.11 Hz, 1 H), 3.51 (q, J = 6.84 Hz, 2 H), 2.83 (t, J = 7.29 Hz, 2 H), 1.47 (s, 9 H).

5-[*N*-(*tert*-Butoxycarbonyl)amino]-*N*-(4-methoxy-β-phenethyl)salicylamide (10d). From compound **8** (0.74 g, 2.9 mmol), EDCI (0.85 g, 4.5 mmol), HOBt (0.6 g, 4.5 mmol), triethylamine (1.65 mL, 11.8 mmol) and 4-methoxyphenethylamine (**9d**) (1.32 g, 9.0 mmol), a similar procedure as that described for **10a** gave pure **10d** (0.64 g, 55%) as a white crystalline solid: mp 159−160 °C; ^{1}H NMR (300 MHz, DMSO-d_6) δ 11.72 (s, 1 H), 9.12 (bs, 1 H), 8.70 (t, J = 5.01 Hz, 1 H), 7.88 (s, 1 H), 7.29 (dd, J = 8.65, 1.50 Hz, 1 H), 7.16 (d, J = 7.74 Hz, 2 H), 6.86 (d, J = 7.29 Hz, 2 H), 6.81 (d, J = 8.65 Hz, 1 H), 3.72 (s, 3 H), 3.47 (q, J = 6.38 Hz, 2 H), 2.77 (t, J = 8.20 Hz, 2 H), 1.46 (s, 9 H).

5-[*N*-(*tert*-Butoxycarbonyl)amino]-*N*-(benzyl)salicylamide (10e). From compound **8** (0.77 g, 3.0 mmol), EDCI (0.85 g, 4.5 mmol), HOBt (0.6 g, 4.5 mmol), triethylamine (1.65 mL, 11.8 mmol) and benzylamine (**9e**) (0.65 mL, 6.0 mmol), a similar procedure as that described for **10a** gave pure **10e** (0.54 g, 53%) as a white crystalline solid: mp 184−185 °C; ^{1}H NMR (300 MHz, DMSO-d_6) δ 11.74 (s, 1 H), 9.15 (bs, 2 H), 7.94 (s, 1 H), 7.41−7.21 (m, 6 H), 6.84 (d, J = 9.11 Hz, 1 H), 4.51 (d, J = 4.10 Hz, 2 H), 1.46 (s, 9 H).

5-[*N*-(*tert*-Butoxycarbonyl)amino]-*N*-(4-chloro-β-phenethyl)salicylamide (10f). From compound **8** (0.61 g, 2.4 mmol), EDCI (0.69 g, 3.6 mmol), HOBt (0.49 g, 3.6 mmol), triethylamine (1.3 mL, 9.2 mmol) and 4-chlorophenethylamine (**9f**) (1.12 g, 7.2 mmol), a similar procedure as that described for **10a** gave pure **10f** (0.55 g, 58%) as a white crystalline solid: mp 192−193 °C; ^{1}H NMR (300 MHz, $CDCl_3$) δ 11.66 (s, 1 H), 9.13 (bs, 1 H), 8.71 (t, J = 5.42 Hz, 1 H), 7.87 (s, 1 H), 7.31 (d, J = 8.39 Hz, 2 H), 7.29 (d, J = 8.21 Hz, 2 H), 7.27 (dd, J = 8.39, 2.04 Hz, 1 H), 6.80 (d, J = 8.77 Hz, 1 H), 3.52 (q, J = 6.17 Hz, 2 H), 2.84 (t, J = 7.06 Hz, 2 H), 1.47 (s, 9 H).

5-[*N*-(*tert*-Butoxycarbonyl)amino]-*N*-(4-hydroxy-β-phenethyl)salicylamide (10g). From compound **8** (0.61 g, 2.4 mmol), EDCI (0.69 g, 3.6 mmol), HOBt (0.49 g, 3.6 mmol), triethylamine (1.3 mL, 9.3 mmol) and 4-hydroxyphenethylamine (**9g**) (1.2 g, 8.7 mmol), a similar procedure as that described for **10a** gave pure **10g** (0.37 g, 42%) as a white crystalline solid: mp 194−195 °C; ^{1}H NMR (300 MHz, DMSO-d_6) δ 11.73 (s, 1 H), 9.19 (s, 1 H), 9.12 (s, 1 H), 8.69 (t, J = 4.51 Hz, 1 H), 7.88 (s, 1 H), 7.31 (d, J = 9.3 Hz, 1 H), 7.05 (d, J = 8.22 Hz, 2 H), 6.82 (d, J = 8.68 Hz, 1 H), 6.68 (d, J = 7.67 Hz, 2 H), 3.43 (q, J = 8.03 Hz, 2 H), 2.72 (t, J = 7.20 Hz, 2 H), 1.46 (s, 9 H).

5-[*N*-(*tert*-Butoxycarbonyl)amino]-*N*-(2-morpholinoethyl)salicylamide (10h). From compound **8** (0.38 g, 1.5 mmol), EDCI (0.43 g, 2.2 mmol), HOBt (0.30 g, 2.2 mmol), triethylamine (0.87 mL, 6.0 mmol) and 4-(2-aminoethyl)-

morpholine (**9h**) (0.39 mL, 3.0 mmol), a similar procedure as that described for **10a** gave pure **10h** (0.33 g, 56%) as a white crystalline solid: mp 154−155 °C; ^{1}H NMR (300 MHz, $CDCl_3$) δ 11.02 (s, 1 H, OH), 7.83 (bs, 1 H, NH), 7.01 (dd, J = 9.82, 2.14 Hz, 1 H), 6.91 (d, J = 9.9 Hz, 1 H), 6.68 (bs, 1 H), 6.50 (d, J = 2.01 Hz, 1 H), 3.56 (t, J = 4.40 Hz, 4 H), 3.47 (m, 4 H), 2.39 (m, 4 H), 1.43 (s, 9 H).

5-[*N*-(*tert*-Butoxycarbonyl)amino]-*N*-(2-pyridin-2-ylethyl)salicylamide (10i). From compound **8** (0.25 g, 0.99 mmol), EDCI (0.28 g, 1.5 mmol), HOBt (0.26 g, 1.5 mmol), triethylamine (0.3 mL, 2.1 mmol) and 2-(2-aminoethyl)pyridine (**9i**) (0.20 mL, 1.7 mmol), a similar procedure as that described for **10a** gave pure **10i** (0.30 g, 85%) as a white crystalline solid: mp 182−184 °C dec; ^{1}H NMR (300 MHz, DMSO-d_6) δ 11.68 (s, 1 H), 9.13 (s, 1 H), 8.53 (d, J = 4.57 Hz, 1 H), 7.88 (s, 1 H), 7.72 (td, J = 7.67, 1.80 Hz, 1 H), 7.30 (d, J = 7.76 Hz, 1 H), 7.23 (m, 2 H), 6.80 (d, J = 8.78 Hz, 1 H), 3.65 (t, J = 7.17 Hz, 2 H), 3.00 (t, J = 7.10 Hz, 2 H), 1.46 (s, 9 H).

5-[*N*-(*tert*-Butoxycarbonyl)amino]-*N*-(3-phenyl-1-propyl)salicylamide (10j). From compound **8** (0.38 g, 1.5 mmol), EDCI (0.43 g, 2.2 mmol), HOBt (0.30 g, 2.2 mmol), triethylamine (0.87 mL, 6 mmol) and 3-phenyl-1-propylamine (**9j**) (0.43 mL, 3.0 mmol), a similar procedure as that described for **10a** gave pure **10j** (0.45 g, 41%) as a white crystalline solid: mp 111−112 °C; ^{1}H NMR (300 MHz, DMSO-d_6) δ 11.85 (s, 1 H), 9.11 (s, 1 H), 8.72 (s, 1 H), 7.75 (s, 1 H), 7.34−7.14 (m, 6 H), 6.82 (d, J = 8.8 Hz, 1 H), 3.27 (t, J = 6.98 Hz, 2 H), 2.59 (t, J = 7.65 Hz, 2 H), 1.80 (quintet, J = 7.15 Hz, 2 H), 1.43 (s, 9 H).

5-[*N*-(*tert*-Butoxycarbonyl)amino]-*N*-(dodecyl)salicylamide (10k). From compound **8** (0.38 g, 1.5 mmol), EDCI (0.43 g, 2.2 mmol), HOBt (0.30 g, 2.2 mmol), triethylamine (0.87 mL, 6 mmol) and dodecylamine (**9k**) (0.55 g, 3.0 mmol), a similar procedure as that described for **10a** gave pure **10k** (0.35 g, 56%) as a white crystalline solid: mp 104−105 °C; ^{1}H NMR (300 MHz, DMSO-d_6) δ 11.89 (s, 1 H), 9.09 (s, 1 H), 7.86 (s, 1 H), 7.28 (d, J = 7.36 Hz, 1 H), 6.81 (d, J = 8.8 Hz, 1 H), 3.25 (t, J = 6.81 Hz, 2 H), 1.46 (s, 9 H), 1.22 (m, 20 H), 0.84 (t, J = 6.73 Hz, 3 H).

5-[*N*-[(*tert*-Butoxycarbonyl)methyl]amino]-*N*-(1,2,3,4-tetrahydronaphthalen-2-yl)salicylamide (10l). From compound **8** (0.40 g, 1.6 mmol), EDCI (0.46 g, 2.4 mmol), HOBt (0.32 g, 2.4 mmol), triethylamine (0.90 mL, 6.3 mmol) and 1,2,3,4-tetrahydronaphthalen-2-amine hydrochloride (**9l**) (0.43 g, 2.3 mmol), a similar procedure as that described for **10a** gave pure **10l** (0.36 g, 59%) as a white crystalline solid: mp 211−212 °C; ^{1}H NMR (300 MHz, DMSO-d_6) δ 11.62 (s, 1 H, OH), 9.11 (s, 1 H, NH), 8.64 (t, J = 7.14 Hz, 1 H), 7.91 (s, 1 H), 7.34 (d, J = 8.71 Hz, 1 H), 7.10 (m, 4 H), 6.82 (d, J = 8.75 Hz, 1 H), 4.23 (m, 1 H), 3.06 (dd, J = 16.19, 4.99 Hz, 1 H), 2.89−2.77 (m, 3 H), 2.06−1.98 (m, 1 H), 1.88−1.75 (m, 1 H), 1.46 (s, 9 H).

4-[*N*-(*tert*-Butoxycarbonyl)amino]-*N*-(3β-cholestanyl)-salicylamide (10m). From compound **8** (0.20 g, 0.8 mmol), EDCI (0.23 g, 1.2 mmol), HOBt (0.16 g, 1.2 mmol), triethylamine (0.44 mL, 3.2 mmol) and 3β-aminocholestane hydrochloride (**9m**) (0.35 g, 0.82 mmol), a similar procedure as that described for **10a** gave pure **10m** (0.31 g, 62%) as a white crystalline solid: mp 230−231 °C dec; ^{1}H NMR (300 MHz, $CDCl_3$) δ 12.36 (s, 1 H, OH), 7.77 (bs, 1 H, NH), 7.26 (s, 1 H), 7.01 (dd, J = 8.88, 2.92 Hz, 1 H), 6.90 (d, J = 8.75 Hz, 1 H), 6.36 (bs, 1 H, NH), 3.95 (m, 1 H), 1.99−1.67 (m, 3 H), 1.63 (d, J = 2.78 Hz, 4 H), 1.52 (s, 9 H), 1.47−0.99 (m, 9 H), 0.91 (d, J = 6.47 Hz, 3 H), 0.87 (dd, J = 6.59, 1.26 Hz, 6 H), 0.81 (s, 3 H), 0.65 (s, 3 H).

5-Amino-*N*-(β-phenethyl)salicylamide (11a). A solution of **10a** (1.0 g, 2.8 mmol) in 6:1 dichloromethane:trifluoroacetic acid (9 mL) was stirred at room temperature for 2 h. The solvent was evaporated in vacuo, and diethyl ether (20 mL) was added. The precipitate was collected, washed with ether and dried to provide white solid **11a** (0.72 g, 100%): mp 190−191 °C; ^{1}H NMR (300 MHz, DMSO-d_6) δ 8.73 (t, J = 1.8 Hz, 1 H), 7.67 (d, J = 2.74 Hz, 1 H), 7.35−7.20 (m, 6 H), 7.03 (d, J = 8.77 Hz, 1 H), 3.54 (q, J = 6.47 Hz, 2 H), 2.86 (t, J = 7.12 Hz, 2 H).

5-Amino-*N*-(4-fluoro-β-phenethyl)salicylamide (11b). From compound **10b** (0.56 g, 1.5 mmol), a similar procedure as that described for **11a** provided white solid **11b** (0.43 g, 104%): mp 200−202 °C dec; ^{1}H NMR (300 MHz, DMSO-d_6) δ 11.9 (bs, 1 H), 9.83 (bs, 1 H), 8.73 (t, J = 5.50 Hz, 1 H), 7.71 (d, J = 2.54 Hz, 1 H), 7.31−7.26 (m, 2 H), 7.23 (d, J = 2.67 Hz, 1 H), 7.12 (t, J = 8.93 Hz, 1 H), 7.02 (d, J = 8.77 Hz, 1 H), 3.54 (q, J = 6.90 Hz, 2 H), 2.84 (t, J = 7.15 Hz, 2 H).

5-Amino-*N*-(4-bromo-β-phenethyl)salicylamide (11c). From compound **10c** (0.54 g, 1.2 mmol), a similar procedure as that described for **11a** provided white solid **11c** (0.41 g, 101%): mp 201−202 °C dec; ^{1}H NMR (300 MHz, DMSO-d_6) δ 12.48 (bs, 1 H), 9.27 (bs, 2 H), 8.73 (t, J = 5.78 Hz, 1 H), 7.77 (d, J = 2.90 Hz, 1 H), 7.49 (d, J = 8.35 Hz, 2 H), 7.27 (dd, J = 9.08, 2.54 Hz, 1 H), 7.23 (d, J = 8.36 Hz, 2 H), 7.00 (d, J = 8.72 Hz, 1 H), 3.55 (q, J = 6.18 Hz, 2 H), 2.84 (t, J = 7.26 Hz, 2 H).

5-Amino-*N*-(4-methoxyphenethyl)salicylamide (11d). From compound **10d** (0.64 g, 1.65 mmol), a similar procedure as that described for **11a** provided white solid **11d** (0.48 g, 100%): mp 196−198 °C dec; ^{1}H NMR (300 MHz, DMSO-d_6) δ 12.03 (bs, 1 H), 9.40 (bs, 2 H), 8.74 (t, J = 5.73 Hz, 1 H), 7.74 (d, J = 2.86 Hz, 1 H), 7.28 (dd, J = 9.06, 2.87 Hz, 1 H), 7.18 (d, J = 8.58 Hz, 2 H), 7.00 (d, J = 8.59 Hz, 1 H), 6.87 (d, J = 8.58 Hz, 2 H), 3.73 (s, 3 H), 3.52 (q, J = 6.19 Hz, 2 H), 2.79 (t, J = 7.63 Hz, 2 H).

5-Amino-*N*-(benzyl)salicylamide (11e). From compound **10e** (0.53 g, 1.55 mmol), a similar procedure as that described for **11a** provided white solid **11e** (0.38 g, 101%): mp 202−204 °C dec; ^{1}H NMR (300 MHz, DMSO-d_6) δ 12.27 (bs, 1 H), 9.40 (m, 2 H), 9.18 (t, J = 5.80 Hz, 1 H), 7.73 (s, 1 H), 7.35 (d, J = 1.78 Hz, 1 H), 7.37−7.20 (m, 5 H), 7.00 (d, J = 8.46 Hz, 1 H), 4.54 (d, J = 5.79 Hz, 2 H).

5-Amino-*N*-(4-chloro-β-phenethyl)salicylamide (11f). From compound **10f** (0.46 g, 1.18 mmol), a similar procedure as that described for **11a** provided white solid **11f** (0.34 g, 100%): mp 199−200 °C dec; ^{1}H NMR (300 MHz, DMSO-d_6) δ 12.48 (bs, 1 H), 9.33 (bs, 2 H), 8.73 (t, J = 5.01 Hz, 1 H), 7.70 (d, J = 2.80 Hz, 1 H), 7.36 (d, J = 8.19 Hz, 2 H), 7.28 (d, J = 8.09 Hz, 2 H), 7.26 (dd, J = 9.21, 2.51 Hz, 1 H), 6.98 (d, J = 8.68 Hz, 1 H), 3.54 (q, J = 6.10 Hz, 2 H), 2.85 (t, J = 7.00 Hz, 2 H).

5-Amino-*N*-(4-hydroxy-β-phenethyl)salicylamide (11g). From compound **10g** (0.35 g, 0.94 mmol), a similar procedure as that described for **11a** provided white solid **11g** (0.25 g, 100%): mp 139−140 °C dec; ^{1}H NMR (300 MHz, CD_3OD) δ 7.82 (d, J = 2.65 Hz, 1 H), 7.34 (dd, J = 8.71, 2.69 Hz, 1 H), 7.08 (d, J = 8.02 Hz, 2 H), 7.02 (d, J = 8.76 Hz, 1 H), 3.60 (t, J = 7.13 Hz, 2 H), 2.81 (t, J = 7.02 Hz, 2 H).

5-Amino-*N*-(2-morpholinoethyl)salicylamide (11h). From compound **10h** (0.30 g, 0.82 mmol), a similar procedure as that described for **11a** provided white solid **11h** (0.21 g, 100%): ^{1}H NMR (300 MHz, $CDCl_3$) δ 10.82 (s, 1 H, OH), 7.83 (bs, 1 H, NH), 7.01 (dd, J = 8.90, 2.14 Hz, 1 H), 6.98 (d, J = 9.01 Hz, 1 H), 6.50 (d, J = 2.01 Hz, 1 H), 3.56 (t, J = 4.20 Hz, 4 H), 3.47 (m, 4 H), 2.39 (m, 4 H).

5-Amino-*N*-(2-pyridin-2-ylethyl)salicylamide (11i). From compound **10i** (0.29 g, 0.81 mmol), a similar procedure as that described for **11a** provided white solid **11i** (0.21 g, 100%): mp 163−165 °C; ^{1}H NMR (300 MHz, DMSO-d_6) δ 12.08 (s, 1 H), 8.85 (t, J = 5.57 Hz, 1 H), 8.69 (d, J = 5.13 Hz, 1 H), 8.11 (td, J = 7.66, 1.67 Hz, 1 H), 7.75 (d, J = 2.67 Hz, 1 H), 7.63 (d, J = 7.92, 1 H), 7.58 (t, J = 6.41 Hz, 1 H), 7.33 (dd, J = 8.71, 2.76 Hz, 1 H), 7.03 (d, J = 8.72 Hz, 1 H), 3.73 (q, J = 5.82 Hz, 2 H), 3.15 (t, J = 6.66 Hz, 2 H).

5-Amino-*N*-(3-phenyl-1-propyl)salicylamide (11j). From compound **10j** (0.35 g, 0.95 mmol), a similar procedure as that described for **11a** provided white solid **11j** (0.23 g, 90%): mp 162−164 °C; ^{1}H NMR (300 MHz, DMSO-d_6) δ 12.10 (bs, 1 H), 8.76 (t, J = 5.52 Hz, 1 H), 7.74 (d, J = 2.69 Hz, 1 H), 7.31−7.02 (m, 6 H), 7.00 (d, J = 8.71 Hz, 1 H), 3.70 (bs, 1 H), 3.32

(q, J = 5.71 Hz, 2 H), 2.63 (t, J = 7.35 Hz, 2 H), 1.84 (quintet, J = 7.37 Hz, 2 H).

5-Amino-*N*-(dodecyl)salicylamide (11k). From compound **10k** (0.35 g, 0.83 mmol), a similar procedure as that described for **11a** provided white solid **11k** (0.27 g, 101%): mp 158−160 °C; ^{1}H NMR (300 MHz, DMSO-d_6) δ 8.70 (s, 1 H), 7.76 (d, J = 2.43 Hz, 1 H), 7.35 (dd, J = 8.72, 2.65 Hz, 1 H), 7.06 (d, J = 8.74 Hz, 1 H), 3.30 (t, J = 6.8 Hz, 2 H), 1.25 (m, 20 H), 0.85 (t, J = 6.64 Hz, 3 H).

5-Amino-*N*-(1,2,3,4-tetrahydronaphthalen-2-yl)salicylamide (11l). From compound **10l** (0.35 g, 0.91 mmol), a similar procedure as that described for **11a** provided white solid **11l** (0.25 g, 98%): mp 208−209 °C dec; ^{1}H NMR (300 MHz, DMSO-d_6) δ 8.67 (d, J = 7.54 Hz, 1 H), 7.75 (d, J = 2.51 Hz, 1 H), 7.25 (dd, J = 8.69, 2.56 Hz, 1 H), 7.10 (m, 4 H), 6.98 (d, J = 8.72 Hz, 1 H), 4.25 (m, 1 H), 3.09 (dd, J = 16.46, 5.29 Hz, 1 H), 2.89−2.76 (m, 3 H), 2.03 (m, 1 H), 1.89−1.79 (m, 1 H).

5-Amino-*N*-(3β-cholestanyl)salicylamide (11m). From compound **10m** (0.29 g, 0.46 mmol), a similar procedure as that described for **11a** provided white solid **11m** (0.21 g, 87%): mp 200−202 °C dec; ^{1}H NMR (300 MHz, DMSO-d_6) δ 12.18 (bs, 1 H, OH), 8.51 (d, J = 7.73 Hz, 1 H), 7.73 (d, J = 2.46 Hz, 1 H), 7.26 (dd, J = 8.72, 2.56 Hz, 1 H), 6.98 (d, J = 8.74 Hz, 1 H), 1.94−0.98 (m, 20 H), 0.88 (d, J = 6.35 Hz, 3 H), 0.83 (d, J = 6.65 Hz, 6 H), 0.80 (s, 3 H), 0.62 (s, 3 H).

5-[*N*-[(2,5-Dihydroxyphenyl)methyl]amino]-*N*-(phenethyl)salicylamide (13a). 2,5-Dihydroxybenzaldehyde **(12)** (0.21 g, 1.40 mmol) was added to **11a** (0.35 g, 1.40 mmol) in benzene (40 mL), and the mixture was heated to reflux under argon for 24 h, using a Dean−Stark trap. The reaction mixture was then concentrated to remove the benzene completely, and the residue was redissolved in methanol (15 mL). While stirring, sodium cyanoborohydride $NaBH_3CN$ (0.18 g, 2.81 mmol) was added in three portions during 30 min, and the reaction mixture was stirred at room temperature for an additional 1 h. To the reaction mixture was then added a saturated solution of NaCl (100 mL) containing 37% HCl (0.28 g, 2.8 mmol). The reaction mixture was extracted with ethyl acetate (3 × 50 mL). The combined organic layers were washed with brine (10 mL), dried over sodium sulfate and concentrated to furnish the crude product, which was further purified by flash chromatography (silica gel 40 g, ethyl acetate:hexane 1:1). The product **13a** (0.37 g, 71.4%) was isolated as a light yellow solid: mp 175−177 °C; ^{1}H NMR (300 MHz, DMSO-d_6) δ 11.43 (s, 1 H, OH), 8.76 (m, 2 H, OH, NH), 8.58 (s, 1 H, OH), 7.35−7.20 (m, 5 H), 7.05 (d, J = 2.51, 1 H), 6.74 (dd, J = 2.28, 8.79 Hz, 1 H), 6.68 (d, J = 8.97 Hz, 1 H), 6.66 (d, J = 3.53 Hz, 1 H), 6.63 (d, J = 8.56 Hz, 1 H), 6.46 (dd, J = 2.75, 8.58 Hz, 1 H), 5.43 (bs, 1 H, NH), 4.11 (s, 2 H), 3.52 (q, J = 6.52 Hz, 2 H), 2.86 (t, J = 7.19 Hz, 2 H); FABMS (Gly) m/z 379 (MH^+). Anal. ($C_{22}H_{22}N_2O_4$) C, H, N.

5-[*N*-[(2,5-Dihydroxyphenyl)methyl]amino]-*N*-(4-fluorophenethyl)salicylamide (13b). From compounds **11b** (0.56 g, 2.0 mmol), **12** (0.35 g, 2.5 mmol), and $NaBH_3CN$ (0.26 g, 4.1 mmol), a similar procedure as that described for **13a** gave pure **13b** (0.34 g, 42%) as a slightly yellow crystalline solid: mp 154−156 °C; ^{1}H NMR (300 MHz, $CDCl_3$) δ 11.37 (s, 1 H), 8.77 (s, 1 H), 8.72 (t, J = 5.33 Hz, 1 H), 8.56 (s, 1 H), 7.27 (t, J = 7.07 Hz, 2 H), 7.10 (t, J = 8.92 Hz, 2 H), 7.00 (d, J = 2.78 Hz, 1 H), 6.74 (dd, J = 8.68, 2.61 Hz, 1 H), 6.67 (d, J = 9.09 Hz, 1 H), 6.62 (s, 1 H), 6.59 (d, J = 8.62 Hz, 1 H), 6.42 (dd, J = 8.44, 2.85 Hz, 1 H), 5.42 (bs, 1 H, NH), 4.09 (d, J = 3.88 Hz. 2 H), 3.47 (q, J = 5.92 Hz, 2 H), 2.82 (t, J = 7.08 Hz, 2 H); ESMS m/z 419 (MNa^+), 397 (MH^+). Anal. ($C_{22}H_{21}FN_2O_4$) C, H, N, F.

5-[*N*-[(2,5-Dihydroxyphenyl)methyl]amino]-*N*-(4-bromo-β-phenethyl)salicylamide (13c). From compounds **11c** (0.48 g, 1.4 mmol), **12** (0.24 g, 1.4 mmol) and $NaBH_3CN$ (0.20 g, 2.9 mmol), a similar procedure as that described for **13a** gave pure **13c** (0.42 g, 64%) as a white crystalline solid: mp 179−180 °C; ^{1}H NMR (300 MHz, $CDCl_3$) δ 11.35 (s, 1 H), 8.77 (s, 1 H), 8.71 (t, J = 2.44 Hz, 1 H), 8.56 (s, 1 H), 7.48 (d, J = 8.20 Hz, 2 H), 7.21 (d, J = 8.28 Hz, 2 H), 7.00 (d, J = 2.87, 1 H), 6.72 (dd, J = 8.55, 2.40 Hz, 1 H), 6.67 (d, J = 9.37 Hz, 1 H), 6.60 (s, 1 H), 6.61 (d, J = 9.76 Hz, 1 H), 6.44 (dd, J = 8.40, 2.65 Hz, 1 H), 5.43 (bs, 1 H, NH), 4.09 (d, J = 4.68 Hz, 2 H), 3.49 (q, J = 7.22 Hz, 2 H), 2.81 (t, J = 7.15 Hz, 2 H); ESMS m/z 458 (M^+ + 2), 457 (M^+ + 1), 456 (M^+). Anal. ($C_{22}H_{21}BrN_2O_4$) C, H, N, Br.

5-[*N*-[(2,5-Dihydroxyphenyl)methyl]amino]-*N*-(4-methoxy-β-phenethyl)salicylamide (13d). From compounds **11d** (0.60 g, 2.0 mmol), **12** (0.35 g, 2.5 mmol) and $NaBH_3CN$ (0.25 g, 4.0 mmol), a similar procedure as that described for **13a** gave pure **13d** (0.50 g, 61%) as a white crystalline solid: mp 173−174 °C dec; ^{1}H NMR (300 MHz, DMSO-d_6) δ 11.42 (s, 1 H, OH), 8.78 (s, 1 H, OH), 8.71 (t, J = 5.42 Hz, 1 H, NH), 8.57 (s, 1 H, OH), 7.15 (d, J = 8.60, 2 H), 7.02 (d, J = 2.41 Hz, 1 H), 6.85 (d, J = 8.64 Hz, 2 H), 6.72 (dd, J = 8.76, 2.57 Hz, 1 H), 6.65 (d, J = 8.88 Hz, 1 H), 6.63 (d, J = 3.03 Hz, 1 H), 6.60 (d, J = 8.53 Hz, 1 H), 6.44 (dd, J = 8.48, 2.88 Hz, 1 H), 5.42 (t, J = 5.68 Hz, 1 H, NH), 4.10 (d, J = 4.82 Hz, 2 H), 3.72 (s, 3 H), 3.46 (q, J = 6.91 Hz, 2 H), 2.76 (t, J = 7.02 Hz, 2 H); ESMS m/z 431 (MNa^+), 409 (MH^+). Anal. ($C_{23}H_{24}N_2O_5$) C, H, N.

5-[*N*-[(2,5-Dihydroxyphenyl)methyl]amino]-*N*-(benzyl)salicylamide (13e). From compounds **12** (0.38 g, 2.6 mmol), **11e** (0.54 g, 2.2 mmol) and $NaBH_3CN$ (0.14 g, 2.2 mmol), a similar procedure as that described for **13a** gave pure **13e** (0.55 g, 69%) as a white crystalline solid: mp 195−196 °C; ^{1}H NMR (300 MHz, DMSO-d_6) δ 11.43 (s, 1 H), 9.18 (t, J = 6.24 Hz, 1 H), 8.75 (s, 1 H), 8.56 (s, 1 H), 7.38−7.20 (m, 5 H), 7.09 (d, J = 2.69 Hz, 1 H), 6.76 (dd, J = 8.46, 2.66 Hz, 1 H), 6.68 (d, J = 8.91 Hz, 1 H), 6.65 (d, J = 3.11 Hz, 1 H), 6.60 (d, J = 8.46 Hz, 1 H), 6.43 (dd, J = 8.46, 3.12 Hz, 1 H), 5.41 (t, J = 5.41 Hz, 1 H), 4.49 (d, J = 5.79, 2 H), 4.09 (d, J = 5.35 Hz, 2 H); CIMS m/z 379 (MH^+). Anal. ($C_{21}H_{20}N_2O_4$) C, H, N.

5-[*N*-[(2,5-Dihydroxyphenyl)methyl]amino]-*N*-(4-chloro-β-phenethyl)salicylamide (13f). From compounds **11f** (0.34 g, 1.2 mmol), **12** (0.16 g, 1.2 mmol) and $NaBH_3CN$ (0.15 g, 2.4 mmol), a similar procedure as that described for **13a** gave pure **13f** (0.34 g, 69%) as a light yellow crystalline solid: mp 158−160 °C; ^{1}H NMR (300 MHz, DMSO-d_6) δ 11.35 (s, 1 H, OH), 8.77 (s, 1 H, OH), 8.71 (t, J = 5.31 Hz, 1 H, NH), 8.56 (s, 1 H, OH), 7.48 (d, J = 8.20 Hz, 2 H), 7.21 (d, J = 8.28 Hz, 2 H), 7.00 (d, J = 2.87, 1 H), 6.72 (dd, J = 8.55, 2.40 Hz, 1 H), 6.67 (d, J = 9.37 Hz, 1 H), 6.60 (s, 1 H), 6.61 (d, J = 9.76 Hz, 1 H), 6.44 (dd, J = 8.40, 2.65 Hz, 1 H), 5.44 (t, J = 5.29 Hz, 1 H, NH), 4.09 (d, J = 4.68 Hz, 2 H), 3.49 (q, J = 7.22 Hz, 2 H), 2.81 (t, J = 7.15 Hz, 2 H); ESMS m/z 414 (M^+ + 2), 412 (M^+). Anal. ($C_{22}H_{21}ClN_2O_4$) C, H, N, Cl.

5-[*N*-[(2,5-Dihydroxyphenyl)methyl]amino]-*N*-(4-hydroxyphenethyl)salicylamide (13g). From compounds **11g** (0.22 g, 0.81 mmol), **12** (0.14 g, 0.97 mmol) and $NaBH_3CN$ (0.15 g, 2.3 mmol), a similar procedure as that described for **13a** gave pure **13g** (0.18 g, 55%) as a slightly yellow crystalline solid: mp 175−176 °C; ^{1}H NMR (300 MHz, DMSO-d_6) δ 11.38 (s, 1 H, OH), 9.87 (s, 1 H, OH), 8.76 (s, 1 H, OH), 8.68 (t, J = 5.33 Hz, 1 H, NH), 8.56 (s, 1 H, OH), 7.30 (t, J = 7.07 Hz, 2 H), 7.10 (t, J = 8.92 Hz, 1 H), 7.00 (d, J = 2.78 Hz, 1 H), 6.73 (dd, J = 8.68, 2.61 Hz, 1 H), 6.67 (d, J = 9.09 Hz, 2 H), 6.62 (d, J = 2.50 Hz, 1 H), 6.59 (d, J = 8.62 Hz, 1 H), 6.42 (dd, J = 8.44, 2.85 Hz, 1 H), 5.40 (bs, 1 H, NH), 4.11 (d, J = 3.88 Hz, 2 H), 3.47 (q, J = 5.92 Hz, 2 H), 2.82 (t, J = 7.08 Hz, 2 H); ESMS m/z 417 (MNa^+), 395 (MH^+). Anal. ($C_{22}H_{22}N_2O_5$) C, H, N.

5-[*N*-[(2,5-Dihydroxyphenyl)methyl]amino]-*N*-(2-morpholinoethyl)salicylamide (13h). From compounds **12** (0.12 g, 0.80 mmol), **11h** (0.20 g, 0.75 mmol) and $NaBH_3CN$ (0.19 g, 3.0 mmol), a similar procedure as that described for **13a** gave pure **13h** (0.18 g, 55%) as a yellow crystalline solid: mp 184−186 °C dec; ^{1}H NMR (300 MHz, DMSO-d_6) δ 11.25 (s, 1 H, OH), 8.77 (s, 1 H, OH), 8.66 (t, J = 4.39 Hz, 1 H, NH), 8.55 (s, 1 H, OH), 7.02 (d, J = 2.21 Hz, 1 H), 6.74 (dd, J = 8.80, 2.55 Hz, 1 H), 6.67 (d, J = 8.00 Hz, 1 H), 6.63 (d, J = 2.87 Hz, 1 H), 6.60 (d, J = 8.66 Hz,1 H), 6.43 (dd, J = 8.42, 2.85 Hz, 1 H), 5.45 (s, 1 H, NH), 4.08 (s, 2 H), 3.56 (t, J = 4.42 Hz, 4 H), 3.38 (m, 4 H), 2.43 (m, 4 H); ESMS m/z 388 (MH^+). Anal. ($C_{20}H_{25}N_5O_5$) C, H, N.

5-[*N*-[(2,5-Dihydroxyphenyl)methyl]amino]-*N*-(2-pyridin-2-ylethyl)salicylamide (13i). From compounds **11i** (0.24 g, 0.93 mmol), **12** (0.17 g, 1.2 mmol) and $NaBH_3CN$ (0.25 g, 4.0 mmol), a similar procedure as that described for **13a** gave pure **13i** (0.18 g, 51%) as a white solid: mp 114−116 °C dec; ^{1}H NMR (300 MHz, DMSO-d_6) δ 11.68 (s, 1 H, OH), 9.13 (s, 1 H, OH), 8.79 (m, 2 H), 8.62 (t, J = 2.12 Hz, 1 H, NH), 8.59 (s, 1 H, OH), 8.53 (d, J = 4.67 Hz, 1 H), 7.72 (td, J = 7.67, 1.80 Hz, 1 H), 7.01 (d, J = 2.51 Hz, 1 H), 6.74 (dd, J = 8.87, 2.31 Hz, 1 H), 6.69 (d, J = 8.83 Hz, 1 H), 6.65 (d, J = 2.53 Hz, 1 H), 6.61 (d, J = 8.94 Hz, 1 H), 6.46 (dd, J = 8.61, 2.77 Hz, 1 H), 5.39 (t, J = 1.98 Hz, 1 H, NH), 4.08 (s, 2 H), 3.65 (t, J = 7.20 Hz, 2 H), 3.05 (t, J = 7.31 Hz, 2 H); ESMS m/z 380 (MH^+). Anal. ($C_{21}H_{21}N_3O_4$) C, H, N.

5-[*N*-[(2,5-Dihydroxyphenyl)methyl]amino]-*N*-(3-phenyl-1-propyl)salicylamide (13j). From compounds **12** (0.13 g, 0.98 mmol) **11j** (0.22 g, 0.81 mmol) and $NaBH_3CN$ (0.2 g, 3.1 mmol), a similar procedure as that described for **13a** gave pure **13j** (0.19 g, 60%) as a white crystalline solid: mp 152−154 °C; ^{1}H NMR (300 MHz, DMSO-d_6) δ 11.56 (s, 1 H, OH), 8.77 (s, 1 H, OH), 8.69 (t, J = 4.58 Hz, 1 H, NH), 8.56 (s, 1 H, OH), 7.32−7.16 (m, 5 H), 7.03 (d, J = 2.42 Hz, 1 H), 6.75 (dd, J = 8.82, 2.53 Hz, 1 H), 6.68 (d, J = 8.80 Hz, 1 H), 6.64 (d, J = 2.90 Hz, 1 H), 6.62 (d, J = 8.59 Hz, 1 H), 6.45 (dd, J = 8.53, 2.94 Hz, 1 H), 5.40 (t, J = 5.78 Hz, 1 H, NH), 4.10 (d, J = 4.51 Hz, 2 H), 3.29 (q, J = 4.87 Hz, 2 H), 2.62 (t, J = 7.53 Hz, 2 H), 1.83 (quintet, J = 7.26 Hz, 2 H); CIMS m/z 393 (MH^+). Anal. ($C_{23}H_{24}N_2O_4$) C, H, N.

5-[*N*-[(2,5-Dihydroxyphenyl)methyl]amino]-*N*-(dodecyl)-salicylamide (13k). From compounds **11k** (0.30 g, 0.93 mmol), **12** (0.14 g, 1.0 mmol) and $NaBH_3CN$ (0.13 g, 2.0 mmol), a similar procedure as that described for **13a** gave pure **13k** (0.23 g, 56%) as a slightly yellow crystalline solid: mp 126−128 °C; ^{1}H NMR (300 MHz, DMSO-d_6) δ 11.59 (s, 1 H, OH), 8.77 (s, 1 H, OH), 8.62 (t, J = 2.12 Hz, 1 H, NH), 8.56 (s, 1 H, OH), 7.01 (d, J = 2.51 Hz, 1 H), 6.74 (dd, J = 8.87, 2.31 Hz, 1 H), 6.69 (d, J = 8.83 Hz, 1 H), 6.65 (d, J = 2.53 Hz, 1 H), 6.61 (d, J = 8.94 Hz, 1 H), 6.46 (dd, J = 8.61, 2.77 Hz, 1 H), 5.39 (t, J = 1.98 Hz, 1 H, NH), 4.09 (s, 2 H), 3.25 (t, J = 7.90 Hz, 2 H), 1.50 (m, 2 H), 1.20 (s, 18 H), 0.88 (t, J = 6.87 Hz, 3 H); CIMS m/z 443 (MH^+). Anal. ($C_{26}H_{38}N_2O_4$) C, H, N.

5-[*N*-[(2,5-Dihydroxyphenyl)methyl]amino]-*N*-(1,2,3,4-tetrahydronaphthalen-2-yl)salicylamide (13l). From compounds **11l** (0.32 g, 1.13 mmol), **12** (0.19 g, 1.36 mmol) and $NaBH_3CN$ (0.3 g, 4.7 mmol), a similar procedure as that described for **13a** gave pure **13l** (0.28 g, 61%) as a yellow crystalline solid: mp 159−161 °C; ^{1}H NMR (300 MHz, DMSO-d_6) δ 11.30 (s, 1 H, OH), 8.79 (s, 1 H, OH), 8.62 (t, J = 4.58, 1 H, NH), 8.58 (s, 1 H, OH), 7.11 (m, 5 H), 6.74 (dd, J = 8.83, 2.41 Hz, 1 H), 6.67 (d, J = 8.87 Hz, 1 H), 6.65 (d, J = 2.82 Hz, 1 H), 6.60 (d, J = 8.49 Hz, 1 H), 6.45 (dd, J = 8.44, 2.84 Hz, 1 H), 5.45 (t, J = 5.30 Hz, 1 H, NH), 4.22 (m, 1 H), 4.11 (d, J = 4.51 Hz, 2 H), 3.07 (dd, J = 16.34, 5.10 Hz, 1 H), 2.89−2.76 (m, 3 H), 2.03 (m, 1 H), 1.80 (m, 1 H); CIMS m/z 405 (MH^+). Anal. ($C_{24}H_{24}N_2O_4$) C, H, N.

5-[*N*-[(2,5-Dihydroxyphenyl)methyl]amino]-*N*-(3β-cholestanyl)salicylamide (13m). From compounds **11m** (0.15 g, 0.28 mmol), **12** (0.05 g, 0.35 mmol) and $NaBH_3CN$ (0.14 g, 2.2 mmol), a similar procedure as that described for **13a** gave pure **13m** (0.08 g, 44%) as a yellow solid: mp 202−204 °C dec; ^{1}H NMR (300 MHz, DMSO-d_6) δ 11.65 (s, 1 H, OH), 8.79 (s, 1 H, OH), 8.58 (s, 1 H, OH), 8.38 (d, 1 H, NH), 7.04 (d, J = 2.16 Hz, 1 H), 6.72 (dd, J = 8.81, 2.18 Hz, 1 H), 6.66−6.64 (m, 2 H), 6.59 (d, J = 8.56 Hz, 1 H), 6.45 (dd, J = 8.50, 2.70 Hz, 1 H), 5.35 (bs, 1 H, NH), 4.09 (s, 2 H), 3.81 (m, 1 H), 1.95−1.00 (m, 21 H), 0.90 (d, J = 6.34 Hz, 3 H), 0.86 (dd, J = 6.66, 1.17 Hz, 6 H), 0.82 (s, 3 H), 0.63 (s, 3 H); CIMS m/z 646 (MH^+). Anal. ($C_{41}H_{60}N_2O_4$) C, H, N.

4-[(*tert*-Butoxycarbonyl)amino]benzoic Acid (15). From 4-aminobenzoic acid (**14**) (0.5 g, 3.65 mmol), triethylamine (1.02 mL, 7.30 mmol) and di-*tert*-butyl dicarbonate (1.59 g, 7.30 mmol), a similar procedure as that described for **8** provided pure **15** (0.86 g, 100%) as a white solid: mp 191−192 °C; ^{1}H NMR (300 MHz, DMSO-d_6) δ 9.71 (s, 1 H), 7.82 (d, J = 8.64 Hz, 2 H), 7.54 (d, J = 8.68 Hz, 2 H), 1.47 (s, 9 H).

4-[*N*-(*tert*-Butoxycarbonyl)amino]-*N*-(benzyl)benzamide (16a). From compound **15** (0.38 g, 1.5 mmol), EDCI (0.43 g, 2.2 mmol), HOBt (0.30 g, 2.2 mmol), triethylamine (0.87 mL, 6.0 mmol) and benzylamine (**9e**) (0.33 mL, 3.0 mmol), a similar procedure as that described for **10a** gave pure **16a** (0.34 g, 69%) as a white crystalline solid: mp 198−199 °C; ^{1}H NMR (300 MHz, $CDCl_3$) δ 7.74 (d, J = 8.58 Hz, 2 H), 7.43 (d, J = 8.55 Hz, 2 H), 7.37−7.26 (m, 5 H), 4.64 (d, J = 5.63 Hz, 2 H), 1.52 (s, 9 H).

4-[*N*-(*tert*-Butoxycarbonyl)amino]-*N*-(β-phenethyl)benzamide (16b). From compound **15** (0.278 g, 1.16 mmol), EDCI (0.45 g, 2.34 mmol), HOBt (0.32 g, 2.34 mmol), triethylamine (0.36 mL, 4.68 mmol) and β-phenethylamine (**9a**) (1.0 mL, 11.7 mmol), a similar procedure as that described for **10a** gave pure **16b** (0.23 g, 58%) as a white crystalline solid: mp 210−211 °C; ^{1}H NMR (300 MHz, $CDCl_3$) δ 7.64 (d, J = 8.69 Hz, 2 H), 7.40 (d, J = 8.65 Hz, 2 H), 7.36−7.22 (m, 5 H), 6.62 (s, 1 H), 6.05 (t, J = 6.5 Hz, 1 H), 3.71 (q, J = 6.8 Hz, 2 H), 2.93 (t, J = 6.9 Hz, 2 H), 1.52 (s, 9 H).

4-[*N*-(*tert*-Butoxycarbonyl)amino]-*N*-(3-phenyl-1-propyl)benzamide (16c). From compound **15** (0.38 g, 1.5 mmol), EDCI (0.43 g, 2.2 mmol), HOBt (0.30 g, 2.2 mmol), triethylamine (0.87 mL, 6.0 mmol) and 3-phenyl-1-propylamine (**9j**) (0.43 mL, 3.0 mmol), a similar procedure as that described for **10a** gave pure **16c** (0.43 g, 81%) as a white crystalline solid: mp 178−180 °C; ^{1}H NMR (300 MHz, $CDCl_3$) δ 7.61 (d, J = 8.69 Hz, 2 H), 7.42 (d, J = 8.70 Hz, 2 H), 7.33−7.19 (m, 5 H), 4.69 (q, J = 6.19 Hz, 2 H), 2.73 (t, J = 7.28 Hz, 2 H), 1.97 (quint, J = 7.47 Hz, 2 H), 1.53 (s, 9 H).

4-Amino-*N*-(benzyl)benzamide (17a). From compound **16a** (0.30 g, 0.92 mmol), a similar procedure as that described for **11a** provided white solid **17a** (0.20 g, 100%): mp 199−200 °C dec; ^{1}H NMR (300 MHz, DMSO-d_6) δ 8.67 (t, J = 5.66 Hz, 1 H, NH), 7.70 (d, J = 8.57 Hz, 2 H), 7.34−7.20 (m, 5 H), 6.71 (d, J = 8.52 Hz, 2 H), 5.11 (bs, 2 H, NH_2), 4.44 (d, J = 4.22 Hz, 2 H).

4-Amino-*N*-(β-phenethyl)benzamide (17b). From compound **16b** (0.066 g, 0.19 mmol), a similar procedure as that described for **11a** provided **17b** (0.045 g, 98.6%) as a white solid: ^{1}H NMR (300 MHz, $CDCl_3$) δ 7.54 (d, J = 8.51 Hz, 2 H), 7.35−7.24 (m, 5 H), 6.65 (d, J = 8.44 Hz, 2 H), 6.15 (bs, 1 H), 4.46 (bs, 2 H), 3.68 (q, J = 6.32 Hz, 2 H), 2.92 (t, J = 6.80 Hz, 2 H).

4-Amino-*N*-(3-phenyl-1-propyl)benzamide (17c). From compound **16c** (0.43 g, 0.92 mmol), a similar procedure as that described for **11a** provided **17c** (0.23 g, 100%) as a white solid: mp 126−128 °C; ^{1}H NMR (300 MHz, DMSO-d_6) δ 8.11 (t, J = 5.25 Hz, 1 H, NH), 7.64 (d, J = 8.59 Hz, 2 H), 7.30−7.17 (m, 5 H), 6.71 (d, J = 8.55 Hz, 2 H), 5.51 (bs, 2 H, NH_2), 3.23 (q, J = 7.04 Hz, 2 H), 2.60 (t, J = 7.39 Hz, 2 H), 1.81 (quint, J = 7.21 Hz, 2 H).

4-[*N*-[(2,5-Dihydroxyphenyl)methyl]amino]-*N*-(benzyl)benzamide (18a). From compounds **12** (0.17 g, 1.25 mmol), **17a** (0.34 g, 1.04 mmol) and $NaBH_3CN$ (0.26 g, 4.2 mmol), a similar procedure as that described for **13a** gave pure **18a** (0.28 g, 77%) as a slightly yellow crystalline solid: mp 204−205 °C; ^{1}H NMR (300 MHz, DMSO-d_6) δ 8.81 (s, 1 H, OH), 8.57 (t, J = 3.79 Hz, 1 H, NH), 8.57 (s, 1 H, OH), 7.65 (d, J = 8.72 Hz, 2 H), 7.32−7.18 (m, 6 H), 6.63 (d, J = 8.37 Hz, 1 H), 6.58 (d, J = 2.76 Hz, 1 H), 6.55 (d, J = 8.72 Hz, 2 H), 6.44 (dd, J = 8.46, 2.81 Hz, 1 H), 4.43 (d, J = 5.88 Hz, 2 H), 4.16 (s, 2 H); CIMS m/z 349 (MH^+). Anal. ($C_{21}H_{20}ClN_2O_3$) C, H, N.

4-[*N*-[(2,5-Dihydroxyphenyl)methyl]amino]-*N*-(β-phenethyl)benzamide (18b). From compounds **12** (0.031 g, 0.22 mmol), **17b** (0.045 g, 0.22 mmol) and $NaBH_3CN$ (0.03 g, 0.47 mmol), a similar procedure as that described for **13a** gave pure **18b** (0.040 g, 59%) as a yellow solid: mp 154−156 °C; ^{1}H NMR (300 MHz, DMSO-d_6) δ 8.81 (s, 1 H, OH), 8.57 (s, 1 H, OH), 8.10 (t, J = 5.38 Hz, 1 H, NH), 7.58 (d, J = 8.41 Hz, 2 H), 7.33−7.17 (m, 6 H), 6.63 (d, J = 8.47 Hz, 1 H), 6.58 (d, J = 2.74 Hz, 1 H), 6.54 (d, J = 8.48 Hz, 2 H), 6.45 (dd, J = 8.47, 2.83 Hz, 1 H), 4.17 (d, J = 4.56 Hz, 2 H), 3.41 (q, J = 8.15 Hz,

2 H), 2.80 (t, J = 7.89 Hz, 2 H); CIMS m/z 363 (MH^+). Anal. ($C_{22}H_{22}N_2O_3$) C, H, N.

4-[*N*-[(2,5-Dihydroxyphenyl)methyl]amino]-*N*-(3-phenyl-1-propyl)benzamide (18c). From compounds **12** (0.17 g, 0.85 mmol), **17c** (0.20 g, 0.8 mmol) and $NaBH_3CN$ (0.21 g, 3.2 mmol), a similar procedure as that described for **13a** gave pure **18c** (0.22 g, 73%) as a slightly yellow crystalline solid: mp 133−134 °C; ^{1}H NMR (300 MHz, DMSO-d_6) δ 8.80 (s, 1 H, OH), 8.57 (s, 1 H, OH), 8.00 (t, J = 5.49 Hz, 1 H, NH), 7.58 (d, J = 8.69 Hz, 2 H), 7.30−7.14 (m, 6 H), 6.62 (d, J = 8.54 Hz, 1 H), 6.57 (d, J = 2.76 Hz, 1 H), 6.53 (d, J = 8.70 Hz, 2 H), 6.42 (dd, J = 8.50, 2.90 Hz, 1 H), 4.15 (s, 2 H), 3.21 (q, J = 6.60 Hz, 2 H), 2.59 (t, J = 7.84 Hz, 2 H), 1.79 (quint, J = 7.55 Hz, 2 H); CIMS m/z 377 (MH^+). Anal. ($C_{23}H_{24}N_2O_3$) C, H, N.

3-[*N*-(*tert*-Butoxycarbonyl)amino]benzoic Acid (20). From 3-aminobenzoic acid (**14**) (0.75 g, 5.47 mmol), triethylamine (1.5 mL, 8.20 mmol) and di-*tert*-butyl dicarbonate (1.78 g, 8.20 mmol), a similar procedure as that described for **8** provided pure **20** (1.3 g, 100%) as a white solid: mp 189−190 °C; ^{1}H NMR (DMSO-d_6) δ 9.53 (s, 1 H), 8.13 (s, 1 H), 7.61 (d, J = 7.66 Hz, 1 H), 7.53 (d, J = 7.52 Hz, 1 H), 7.35 (t, J = 7.91 Hz, 1 H), 1.47 (s, 9 H).

3-[*N*-(*tert*-Butoxycarbonyl)amino]-*N*-(*β*-phenethyl)benzoylamide (21). From compound **20** (0.48 g, 2.03 mmol), EDCI (0.45 g, 2.34 mmol), HOBt (0.33 g, 2.34 mmol), triethylamine (0.37 mL, 4.68 mmol) and *β*-phenethylamine (**9a**), a similar procedure as that described for **10a** gave pure **21** (0.35 g, 51%) as a white solid: mp 186−188 °C; ^{1}H NMR (300 MHz, $CDCl_3$) δ 7.51 (t, J = 4.86 Hz, 1 H), 7.36−7.31 (m, 4 H), 7.24 (d, J = 4.08 Hz, 1 H), 7.22 (d, J = 2.3 Hz, 1 H), 6.61 (s, 1 H), 6.22 (bs, 1 H), 3.71 (q, J = 6.9 Hz, 2 H), 2.93 (t, J = 7.0 Hz, 2 H), 1.53 (s, 9 H).

3-Amino-*N*-(*β*-phenethyl)benzamide (22). From compound **21** (0.23 g, 0.66 mmol), a similar procedure as that described for **11a** provided white solid **22** (0.16 g, 100%): mp 137−139 °C; ^{1}H NMR (300 MHz, DMSO-d_6) δ 8.47 (t, 1 H), 7.35−7.18 (m, 7 H), 6.99 (s, 2 H), 3.46 (q, J = 7.00 Hz, 2 H), 2.83 (t, J = 7.06 Hz, 2 H).

3-[*N*-[(2,5-Dihydroxyphenyl)methyl]amino]-*N*-(*β*-phenethyl)benzamide (23). From compounds **12** (0.25 g, 1.77 mmol), **22** (0.38 g, 1.58 mmol) and $NaBH_3CN$ (0.2 g, 3.16 mmol), a similar procedure as that described for **13a** gave pure **23** (0.42 g, 73%) as a light yellow solid: mp 124−126 °C; ^{1}H NMR (300 MHz, DMSO-d_6) δ 8.81 (s, 1 H, OH), 8.58 (s, 1 H, OH), 8.35 (t, J = 4.93 Hz, 1 H, NH), 7.33−7.19 (m, 5 H), 7.11 (t, J = 7.74 Hz, 1 H), 7.03 (d, J = 2.11 Hz, 1 H), 6.95 (d, J = 7.61 Hz, 1 H), 6.69 (dd, J = 2.24, 8.24 Hz, 1 H), 6.64 (d, J = 8.40 Hz, 1 H), 6.24 (s, 1 H), 6.45 (dd, J = 2.91, 8.28 Hz, 1 H), 6.20 (t, J = 4.56 Hz, 1 H, NH), 4.17 (d, J = 5.46 Hz, 2 H), 3.48 (q, J = 6.55 Hz, 2 H), 2.83 (t, J = 7.67 Hz, 2 H); CIMS m/z 363 (MH^+). Anal. ($C_{22}H_{22}N_2O_3$) C, H, N.

Acknowledgment. This research was made possible by grants from the Showalter Trust, Purdue Research Foundation, National Institutes of Health (CA37372 and CA80770), and American Chemical Society (IRG 58-006-40).

Supporting Information Available: Elemental analyses for compounds **13a**−**m**, **18a**−**c**, and **23**. This material is available free of charge via the Internet at http://pubs.acs.org.

References

(1) Levitzki, A. Protein Tyrosine Kinase Inhibitors as Novel Therapeutic Agents. *Pharmacol. Ther.* **1999**, *82*, 231−239.
(2) Traxler, P.; Furet, R. Strategies Toward the Design of Novel and Selective Protein Tyrosine Kinase Inhibitors. *Pharmacol. Ther.* **1999**, *82*, 195−206.
(3) Hamby, J. M.; Showalter, H. D. Small Molecule Inhibitors of Tumor-Promoted Angiogenesis, Including Protein Tyrosine Kinase Inhibitors. *Pharmacol. Ther.* **1999**, *82*, 169−193.
(4) Onoda, T.; Iinuma, H.; Sasaki, Y.; Hamada, M.; Isshiki, K.; Naganawa, H.; Takeuchi, T. Isolation of a Novel Tyrosine Kinase Inhibitor, Lavendustin A, from *Streptomyces griseolavendus*. *J. Nat. Prod.* **1989**, *52*, 1252−1257.
(5) Hsu, C.-Y. J.; Persons, P. E.; Spada, A. P.; Bednar, R. A.; Levitzki, A.; Zilberstein, A. Kinetic Analysis of the Inhibition of the Epidermal Growth Factor Receptor Tyrosine Kinase by Lavendustin A and Its Analogue. *J. Biol. Chem.* **1991**, *266*, 21105−21112.
(6) Imoto, M.; Sujikai, I.; Ui, H.; Umezawa, K. Involvement of Tyrosine Kinase in Growth Factor-Induced Phospholipase C Activation in NIH3T3 Cells. *Biochim. Biophys. Acta* **1993**, *1166*, 188−192.
(7) Smyth, M. S.; Stefanova, I.; Hartman, F.; Horad, I. D.; Osherov, N.; Levitzki, A. Non-Amine Based Analogues of Lavendustin A as Protein-Tyrosine Kinase Inhibitors. *J. Med. Chem.* **1993**, *36*, 3010−3014.
(8) Smyth, M. S.; Stefanova, I.; Horak, I. D.; Burke, T. R. J. Hydroxylated 2-(5′-Salicyl)naphthalenes as Protein-Tyrosine Kinase Inhibitors. *J. Med. Chem.* **1993**, *36*, 3015−3020.
(9) Chen, H.; Boiziau, J.; Parker, F.; Maroun, R.; Tocque, B.; Roques, B. P.; Garbay-Jaureguiberry, C. Synthesis and Structure−Activity Studies of a Series of [(Hydroxybenzyl)amino]salicylates as Inhibitors of EGF Receptor-Associated Tyrosine Kinase Activity. *J. Med. Chem.* **1993**, *36*, 4094−4098.
(10) Chen, H.; Boiziau, J.; Parker, F.; Mailliet, P.; Commerçon, A.; Tocque, B.; Le Pecq, J.-B.; Roques, B.-P.; Garbay, C. Structure−Activity Relationships in a Series of 5-[(2,5-Dihydroxybenzyl)-amino]salicylate Inhibitors of EGF−Receptor-Associated Tyrosine Kinase: Importance of Additional Hydrophobic Aromatic Interactions. *J. Med. Chem.* **1994**, *37*, 845−859.
(11) Agbotounou, W. K.; Umezawa, K.; Jacuemin-Sablon, A.; Pierre, J. Inhibition by Two Lavendustins of the Tyrosine Kinase Activity of $pp60^{F527}$ In Vitro and in Intact Cells. *Eur. J. Pharmacol.* **1994**, *269*, 1−8.
(12) Nussbaumer, P.; Winiski, A. P.; Cammisuli, S.; Hiestand, P.; Weckbecker, G.; Stütz, A. Novel Antiproliferative Agents Derived from Lavendustin A. *J. Med. Chem.* **1994**, *37*, 4079−4084.
(13) Liu, T.; Shirai, R.; Matsui, T.; Umezawa, K.; Iwasaki, S. Synthesis and Biological Activity of 5-[2,5-Dihydroxybenzyl)-amino]salicylic Acid Analogues as Inhibitors of EGF Receptor-Associated Protein Tyrosine Kinase. *Bioorg. Med. Chem. Lett.* **1997**, *7*, 365−368.
(14) Green, J. Solid-Phase Synthesis of Lavendustin A and Analogues. *J. Org. Chem.* **1995**, *60*, 4287−4290.
(15) Devraj, R.; Cushman, M. A Versatile Solid Phase Synthesis of Lavendustin A and Certain Biologically Active Analogues. *J. Org. Chem.* **1996**, *61*, 9368−9373.
(16) Paull, K. D.; Hamel, E.; Malspeis, L. *Prediction of Biochemical Mechanism of Action from the In Vitro Antitumor Screen of the National Cancer Institute*; American Chemical Society: Washington, DC, 1995.
(17) Paull, K. D.; Shoemaker, R. H.; Hodes, L.; Monks, A.; Scudiero, D. A.; Rubinstein, L.; Plowman, J.; Boyd, M. R. Display and Analysis of Patterns of Differential Activity of Drugs Against Human Tumor Cell Lines: Development of Mean Graph and COMPARE Algorithm. *J. Natl. Cancer Inst.* **1989**, *81*, 1088−1092.
(18) Boyd, M. R.; Paull, K. D. Some Practical Considerations and Applications of the National Cancer Institute In Vitro Anticancer Drug Discovery Screen. *Drug Dev. Res.* **1995**, *34*, 91−109.
(19) Paull, K. D.; Lin, C. M.; Malspeis, L.; Hamel, E. Identification of Novel Antimitotic Agents Acting at the Tubulin Level by Computer-assisted Evaluation of Differential Cytotoxicity Data. *Cancer Res.* **1992**, *52*, 3892−3900.
(20) Kohlhagen, G.; Paull, K.; Cushman, M.; Nagafuji, P.; Pommier, Y. Protein-Linked DNA Strand Breaks Induced by NSC 314622, a Novel Noncamptothecin Topoisomerase I Poison. *Mol. Pharmacol.* **1998**, *54*, 50−58.
(21) Leteurtre, F.; Kohlhagen, G.; Paull, K. D.; Pommier, Y. Topoisomerase II Inhibition and Cytotoxicity of the Anthrapyrazoles DuP 937 and DuP 941 (Losaxantrone) in the National Cancer Institute Preclinical Antitumor Drug Discovery Screen. *J. Natl. Cancer Inst.* **1994**, *86*, 1239−1244.
(22) Cleaveland, E. S.; Monks, A.; Vaigro-Wolff, A.; Zaharevitz, D. W.; Paull, K.; Ardalan, K.; Cooney, D. A.; Ford, H. J. Site of Action of Two Pyrimidine Biosynthesis Inhibitors Accurately Predicted by the COMPARE Program. *Biochem. Pharmacol.* **1995**, *49*, 947−954.
(23) Duncan, K. K.; Duncan, M. D.; Alley, M. C.; Sausville, E. A. Cucurbitacin E-Induced Disruption of the Actin and Vimentin Cytoskeleton in Prostate Carcinoma Cells. *Biochem. Pharmacol.* **1996**, *52*, 1553−1560.
(24) Bubb, M. R.; Senderowicz, A. M.; Sauville, E. A.; Duncan, K. K.; Korn, E. D. Jasplakinolide, a Cytotoxic Natural Product, Induces Actin Polymerization and Competitively Inhibits the Binding of Phalloidin to F-Actin. *J. Biol. Chem.* **1994**, *269*, 14869−14871.
(25) Bradshaw, T. D.; Wrigley, S.; Shi, D.-F.; Schultz, R. J.; Paull, K. D.; Stevens, M. F. G. 2-(4-Aminophenyl)benzothiazoles: Novel Agents with Selective Profiles of In Vitro Antitumor Activity. *Br. J. Cancer* **1998**, *77*, 745−752.

(26) Wosikowski, K.; Schuurhuis, D.; Johnson, K.; Paull, K. D.; Myers, T. G.; Weinstein, J. N.; Bates, S. E. Identification of Epidermal Growth Factor Receptor and C-erb-B2 Pathway Inhibitors by Correlation with Gene Expression Patterns. *J. Natl. Cancer Inst.* **1997**, *89*, 1505−1515.
(27) Riese, D. J. I.; van Raaij, T. M.; Plowman, G. D.; Andrews, G. C.; Stern, D. F. The Cellular Response to Neuregulins is Governed by Complex Interactions of the ErbB Receptor Family. *Mol. Cell. Biol.* **1995**, *15*, 5770−5776.
(28) Normanno, N.; Selvam, M. P.; Qi, C.-F.; Saeki, T.; Johnson, G.; Kim, N.; Ciardiello, F.; Shoyab, M.; Plowman, G.; Brandt, R.; Todaro, G.; Salomon, D. S. Amphiregulin as an Autocrine Growth Factor for C-Ha-*ras*- and c-*erbB-2*-Transformed Human Mammary Epithelial Cells. *Proc. Natl. Acad. Sci. U.S.A.* **1994**, *91*, 2790−2794.
(29) Soule, H. D.; Maloney, T. M.; Wolman, S. R.; Peterson, W. D. J.; Brenz, R.; McGrath, C. M.; Russo, J.; Pauley, R. J.; Jones, R. F.; Brooks, S. C. Isolation and Characterization of a Spontaneously Immortalized Human Breast Epithelial Cell Line, MCF-10. *Cancer Res.* **1990**, *50*, 6075−6086.
(30) Dickstein, B.; Valverius, E. M.; Wosikowski, K.; Saceda, M.; Pearson, J. W.; Martin, M. B.; Bates, S. E. Increased Epidermal Growth Factor Receptor in an Estrogen-responsive, Adriamycin-resistant MCF-7 Cell Line. *J. Cell. Physiol.* **1993**, *157*, 110−118.
(31) Dong, X. F.; Berthois, Y.; Colomb, E.; Martin, P. M. Cell Cycle Phase Dependence of Estrogen and Epidermal Growth Factor (EGF) Receptor Expression in MCF-7 Cells. *Endocrinology* **1991**, *129*, 2719−2728.
(32) Geahlen, R. L.; McLaughlin, J. L. Piceatannol (3,4,3′,5′-Tetrahydroxy-*trans*-stilbene) is a Naturally Occurring Protein Tyrosine Kinase Inhibitor. *Biochem. Biophys. Res. Commun.* **1989**, *165*, 241−245.
(33) Thakkar, K.; Geahlen, R. L.; Cushman, M. Synthesis and Protein-Tyrosine Kinase Inhibitory Activity of Polyhydroxylated Stilbene Analogues of Piceatannol. *J. Med. Chem.* **1993**, *36*, 2950−2955.
(34) Lin, C. M.; Singh, S. B.; Chu, P. S.; Dempcy, R. O.; Schmidt, J. M.; Pettit, G. R.; Hamel, E. Interactions of Tubulin with Potent Natural and Synthetic Analogues of the Antimitotic Agent Combretastatin: a Structure−Activity Study. *Mol. Pharmacol.* **1988**, *34*, 200−208.
(35) Cushman, M.; Nagarathnam, D.; Gopal, D.; Chakraborti, A. K.; Lin, C. M.; Hamel, E. Synthesis and Evaluation of Stilbene and Dihydrostilbene Derivatives as Potential Anticancer Agents that Inhibit Tubulin Polymerization. *J. Med. Chem.* **1991**, *34*, 2579−2588.
(36) Cushman, M.; Nagarathnam, D.; Gopal, D.; He, H.-M.; Lin, C. M.; Hamel, E. Synthesis and Evaluation of Analogues of (Z)-1-(4-Methoxyphenyl)-2-(3,4,5-trimethoxyphenyl)ethene as Potential Cytotoxic and Antimitotic Agents. *J. Med. Chem.* **1992**, *35*, 2293−2306.
(37) Cushman, M.; He, H.-M.; Lin, C. M.; Hamel, E. Synthesis and Evaluation of a Series of Benzylaniline Hydrochlorides as Potential Cytotoxic and Antimitotic Agents Acting by Inhibition of Tubulin Polymerization. *J. Med. Chem.* **1993**, *36*, 2817−2821.
(38) Cammisuli, S.; Winiski, A.; Nussbaumer, P.; Hiestand, P.; Stutz, A.; Weckbecker, G. SDZ 281-977: a Modified Partial Structure of Lavendustin A that Exerts Potent and Selective Antiproliferative Activities In Vitro and In Vivo. *Int. J. Cancer* **1996**, *65*, 351−359.
(39) Hamel, E.; Lin, C. M. Separation of Active Tubulin and Microtubule-Associated Proteins by Ultracentrifugation and Isolation of a Component Causing the Formation of Microtubule Bundles. *Biochemistry* **1984**, *23*, 4173−4184.
(40) Verdier-Pinard, P.; Lai, J. Y.; Yoo, H.-D.; Yu, J.; Marquez, B.; Nagle, D. G.; Nambu, M.; White, J. D.; Falck, J. R.; Gerwick, W. H.; Day, B. W.; Hamel, E. Structure−Activity Analysis of the Interaction of Curacin A, the Potent Colchicine Site Antimitotic Agent, with Tubulin and Effects of Analogues of the Growth of MCF-7 Breast Cancer Cells. *Mol. Pharmacol.* **1998**, *53*, 62−76.
(41) Peters, J. D.; Furlong, M. T.; Asai, D. J.; Harrison, M. L.; Geahlen, R. L. Syk, Activated by Cross-linking the B-cell Antigen Receptor Localizes to the Cytosol Where It Interacts with and Phosphorylates α-Tubulin on Tyrosine. *J. Biol. Chem.* **1996**, *271*, 4755−4762.
(42) Plowman, G. D.; Green, J. M.; Culouscou, J.-M.; Carlton, G. W.; Rothwell, V. M.; Buckley, S. Heregulin Induces Tyrosine Phosphorylation of HER4/p180erbB4. *Nature* **1993**, *366*, 473−475.
(43) Riese, D. J. I.; Komurasaki, T.; Plowman, G. D.; Stern, D. F. Activation of ErbB4 by the Bifunctional EGF Family Hormone Epiregulin is Regulated by ErbB2. *J. Biol. Chem.* **1998**, *273*, 11288−11294.
(44) Hwang, E.-S.; Riese, D. J. I.; Settleman, J.; Nilson, L. A.; Honig, J.; Flynn, S.; DiMaio, D. Inhibition of Cervival Carcinoma Cell Line Proliferation by the Introduction of a Bovine Papillomavirus Regulatory Gene. *J. Virol.* **1993**, *67*, 3720−3729.

JM000387G